Renewable Energy 90 (2016) 399–419

Contents lists available at ScienceDirect

Renewable Energy

journal homepage: www.elsevier.com/locate/renene

10-year high resolution study of wind, sea waves and wave energy assessment in the Greek offshore areas

George Emmanouil [a, b, *], George Galanis [a, b], Christina Kalogeri [c], George Zodiatis [b], George Kallos [c]

[a] Hellenic Naval Academy, Section of Mathematics, Hatzikiriakion, Piraeus 18539, Greece
[b] Oceanography Centre, University of Cyprus, Nicosia 1678, Cyprus
[c] University of Athens, Department of Physics, Atmospheric Modeling and Weather Forecasting Group, University Campus, Bldg. PHYS-V, Athens 15784, Greece

ARTICLE INFO

Article history:
Received 29 May 2015
Received in revised form
29 December 2015
Accepted 6 January 2016
Available online xxx

Keywords:
Sea waves energy
Atmospheric and wave modeling
Wind and wave analysis

ABSTRACT

Nowadays, renewable energy resources are one of the top priority issues for the environmental and political community. In particular, wind and wave energy are two of the most promising solutions, with great potential from research and technological point of view. In this work, an integrated high resolution platform, consisting of state-of-the-art wind-wave numerical models, has been utilized and produced a 10-year database containing all the relevant environmental parameters for a detailed resource assessment over the Greek seas. The results of the atmospheric and sea wave numerical models concerning the environmental parameters that directly affect the wave energy potential were evaluated. High resolution maps for the coastal and offshore areas of Greece present sea wave and wind climatological characteristics, as well as the relevant distribution of the wave energy potential. A number of statistical indices have been employed for analyzing the output of the models, including the potential impact of extreme values and the corresponding distribution of the above parameters, which optimally describe the spatial and temporal analysis of the wave power potential over the area of interest. It is shown that the regions with increased wave energy potential are mainly the western and southern seas of Greece, which are usually exposed to swell from central and south Mediterranean Sea.

© 2016 Elsevier Ltd. All rights reserved.

1. Introduction

A very important issue concerning the scientific and the political community is global warming. A major factor that contributed to these problems is the use of oil-dependent energy resources, which are not environmental friendly. On the other hand, the danger from the nuclear power infrastructures due to natural disasters (earthquakes, extreme weather events) is increased. Both these issues make the necessity of exploring new energy resources more important than ever.

Solar and wind energy are the first of this kind of solution, mostly used until today. Taking into account that 2/3 of the earth is covered by water, sea surfaces may be also used towards this scope. The last years, wave energy combined with wind is investigated by European countries and the US. The energy produced by sea waves has some specific advantages; the most crucial one is the low variability in time compared to the one of wind energy. On the other hand, the technology for exploiting this kind of energy is not at a satisfactory level of progress.

The sea waves energy has been a subject of discussion raised even from the 19th century, as referred to [35]. However, the systematic research in this domain has begun the last twenty years, when the cost of other sources of energy has been raised up and the consequences of the maximization of gas emissions contributed to the global warming effect. Then, several projects involving green energy sources have been supported globally and especially by the European Commission. These projects have been focused in different regions, with different models and statistical tools. Reikard et al. [49] used the ECMWF wave model and some time series methods for forecasting Ocean Wave Energy. Denfe et al. [13] tried to focus their study in the southeast Atlantic coast of the United States based on the measurements of buoy stations. Pontes [45];

* Corresponding author. Hellenic Naval Academy, Section of Mathematics, Hatzikiriakion, Piraeus 18539, Greece.
E-mail address: george.emmanouil@yahoo.gr (G. Emmanouil).

http://dx.doi.org/10.1016/j.renene.2016.01.031
0960-1481/© 2016 Elsevier Ltd. All rights reserved.

presented a European Wave Energy Atlas based on annual and seasonal wave statistics derived from a coarse grid wave modeling simulations and Iglesias et al. [21–23] used hindcast simulated data and buoy measurements for studying the wave energy distribution over different areas of Spain (Death Coast, Galicia and Bares). The area of Azores is discussed in Ref. [50]; when the Black Sea was studied over a 13-year period in Ref. [2] and a 15-year study in Ref. [10]. In the Mediterranean Sea, [54]; studied the area of Sardinia, Italy, based on the Italian buoy network and corresponding hindcast data by ECMWF. More relevant work for the European Atlantic coast has been done by Joana et al. [30] and Gonçalves et al. [19]. Stopa et al. [51] performed a hindcast analysis along the Hawaiian coastline. Chiu et al. [11] focused on wave energy resources in Taiwan and Hughes and Heap [20] presented a study for Australia's shelf waters based on numerical models Finally, Mazarakis et al. [39] focused on validation of WAM (WAve Model) over Ionian and Aegean Seas with buoy and altimeter Jason-2 data, while Ayat [5] studied Mediterranean and Aegean Seas wave power by using MIKE 21 SW and validated the model with 3 buoy stations. Further hindcast studies can be also found in Refs. [42,48].

In this paper, the main meteorological parameters affecting the sea waves' energy potential are studied in detail for the major Greek area, including Aegean and Ionian Seas, for a time period of ten years (2001–2010). A high resolution atmospheric and wave modeling system has been employed in order to simulate wind speed and direction, significant wave height and energy wave period. With these tools, we studied the way that the previous parameters affect the wave energy potential distribution. This system has been operated in a hindcast mode, exploiting the advantages of data assimilation procedure, using the available observations-measurements in this area (satellite records, meteorological observations, buoys). By this way, an optimum representation of the environmental parameters and a detailed wave climatology map of the area have been produced.

The results from these simulations have been elaborated through a detailed statistical analysis, for the meteorological, the sea and the wave energy potential parameters. The statistics refer not only to the usual indices (mean values, standard deviation), but also to asymmetry measures of the results and the impact of possible extreme values. This information could be useful for the site assessment of wave energy devices. On the other hand, probability distribution functions are examined for better description of the main parameters affecting the wave energy potential.

The paper has been organized as follows: In Section 2, the numerical wind and wave models, as well as the way of estimating the wave power potential are presented. In Section 3, the statistical measures used for analyzing the model results and the wave energy related parameters are described. Section 4 contains the discussion of the results, while the conclusions are summarized in Section 5.

2. Models

In this study, the ocean wave model WAM [7,34,53] was used for the simulation of sea wave conditions of the Greek seas for a period of ten years (2001–2010). WAM is a third generation wave model, where the wave transport equation is solved explicitly without any presumptions on the shape of the spectrum. In particular, the ECMWF (European Centre for Medium Range Weather Forecasting) version CY33R1 [6,28] has been employed. A number of improvements have been implemented, like the extension of the advection scheme in the wave energy balance equation for the corner points, using the Corner Transport Upstream scheme, which provides uniform propagation in all directions. Moreover, a new parameterization of shallow water effect, affecting the time evolution of the wave spectrum and the determination of the kurtosis of the wave field [29] has been used. In addition, two extreme wave parameters have been introduced: the average maximum wave height and the corresponding wave energy period [41].

The wave model is calculating the 2-d wave spectrum $F(f, \vartheta, \varphi, \lambda)$, where f stands for frequencies, ϑ for directions, overall latitudes and longitudes (φ, λ) of the domain used. The necessary parameters for this study are obtained as integrated byproducts, based on the moments of the spectrum:

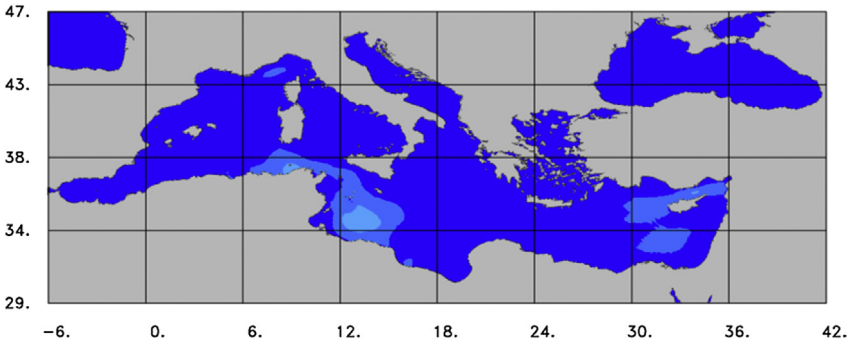

Fig. 1. The simulation area.

Table 1
Summary of the wave model characteristics.

Wave model	WAM, ECMWF version CY33R1
Area covered	29N–47N, 6W–42E
Horizontal resolution	0.05 × 0.05°
Frequencies	25 (range 0.0417–0.54764 Hz logarithmically spaced)
Directions	24 (equally spaced)
Time step	45 s
Wind forcing	SKIRON atmospheric model
Wind forcing time step	3 h

$$m_n = \int_0^{2\pi} \int_0^{\infty} f^n E(f,\theta) df d\theta, \quad n = -1, 0, 1, 2 \tag{1}$$

More precisely, the significant wave height H_s and the energy period T_e are given by

$$H_s = 4\sqrt{m_0}, \quad T_e = \frac{m_{-1}}{m_0} \tag{2}$$

The simulation area is Mediterranean Sea: 29N–47N, 6W–42E (Fig. 1). This was necessary for reproducing swell that affects the west and south parts of the Greek area, which is part of the area of interest. The horizontal resolution is 0.05 × 0.05°, one of the highest used for such studies. In this way, the local characteristics are taken into account in a more detailed way, in contrast to previous wave energy studies, in which much coarser grids were used. For example Pontes [45]; used a 0.5 × 0.5° resolution for the Mediterranean Sea. Arinaga and Cheung [3] employed the WaveWatch3 model with a 1.25 × 1° resolution. In this study, the wave spectrum was discretized to 25 frequencies (range 0.0417–0.54764 Hz logarithmically spaced) and 24 directions (equally spaced), while the propagation time step has been set to 45 s. The main characteristics of the wave model employed are summarized in Table 1.

The necessary atmospheric forcing has been offered in 3-h time intervals from the SKIRON atmospheric model [31,43]. This model has been developed at the National and Kapodestrian University of Athens and it is based on the ETA/National Center for Environmental Prediction (NCEP) model, developed by Refs. [26,40]. The vertical turbulence mixing is performed by mixing coefficients of the modified Mellor-Yamada 2.5 level turbulence. In the surface layer, the Monin–Obukhov similarity theory is used. In order to control the small scale noises, the nonlinear lateral diffusion scheme, with the diffusion coefficient, depending on the deformation and the turbulent kinetic energy was introduced.

The horizontal resolution of the SKIRON model was the same with the wave model. Moreover, 45 vertical levels stretching from surface to 20 Km altitude were employed. The atmospheric system used, for initial and boundary conditions, the NCEP/GFS 0.5 × 0.5° resolution fields. The necessary sea surface boundary conditions were interpolated from the 0.5 × 0.5° SST (Sea Surface Temperature) field analysis retrieved from NCEP on a daily basis. Vegetation and topography data were applied at a resolution of 30 s and soil texture data with resolution of 120 s.

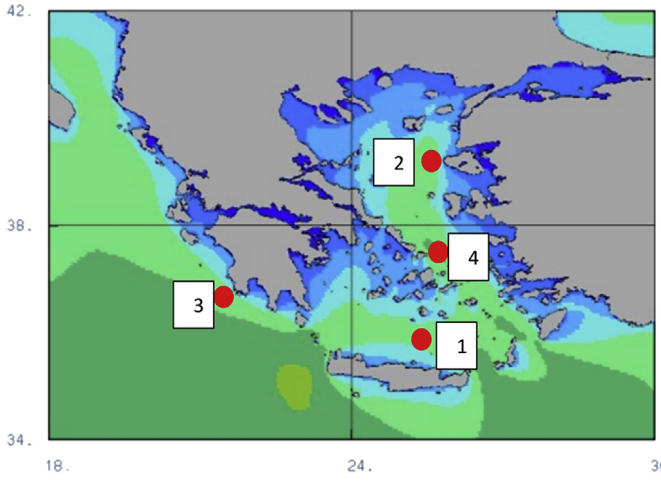

Fig. 2. The four buoy locations used for evaluation.

Table 2
Statistical evaluation for the Cretan, Lesvos, Pylos and Mykonos buoy locations.

	1. Creta, 2007–2010, latitude 35.8N, longitude 24.9E SWH (m)		2. Lesvos, 2006–2010, latitude 39.15N, longitude 25.81E SWH (m)		3. Pylos, 2007–2010, latitude 36.8N, longitude 21.6E SWH (m)		4. Mykonos, 2004–2010, latitude 37.5N, longitude 25.45E SWH (m)	
	Buoy	WAM	Buoy	WAM	Buoy	WAM	Buoy	WAM
Mean	0.92	0.78	0.79	0.73	1.02	0.89	0.99	1.01
St. Dev.	0.62	0.58	0.56	0.58	0.75	0.64	0.73	0.84
Var. Coeff.	0.67	0.74	0.71	0.79	0.74	0.72	0.74	0.83
St. Error	0.01	0.01	0.01	0.01	0.01	0.01	0.01	0.01
Skewness	1.69	2.06	1.51	1.60	1.79	2.01	1.25	1.40
Kurtosis	7.63	9.30	5.94	6.56	7.44	9.49	5.36	5.93

The quality of the atmospheric forcing is very important for the credible simulation by wave models. Several different studies and authors have pointed out this importance (for example Refs. [1,9,16,25,44]). With this aim, any available observations in the study area, obtained by meteorological stations and satellite records for atmospheric and wave parameters have been assimilated into the atmospheric and wave models respectively, based on the standard assimilation schemes of SKIRON and WAM models (see Refs. [12,14,16,27,33,36,47].

More precisely, the data assimilation scheme employed for incorporating into the wave model's integration available buoy and satellite observations is based on an Optimal Interpolation method, as outlined in Ref. [37]. Based on this an analyzed field of significant wave heights is created. In a second step, the two-dimensional wave spectrum is estimated and the information of single wave height measurement is transformed into different corrections for the wind sea and swell parts of the spectrum. More precisely, the.

two-dimensional spectrum is corrected by the introduction of appropriate rescaling factors, derived from duration limited growth relations for the wind sea and swell while it is assumed that the wave steepness is conserved to the energy and frequency scales. On the other hand, the local wind speed forcing is updated. A detailed description of the method can be found in Refs. [14,16,34].

Concerning the atmospheric model, LAPS, a data assimilation system which blends gridded data with existing observations from various sources (ground and remote sensing), has been utilized over a 25 years (1985–2010) reanalysis at a horizontal resolution of 0.15^0 [32].

In order to estimate the wave power potential that can be produced by the local waves, the following formula has been used [55]:

$$P = \frac{\rho_w g^2}{64\pi} T e H_{1/3}^2 \tag{3}$$

where ρ_w is the water density, g the gravity acceleration, $H_{1/3}$ is the significant wave height and T_e is the energy period of the wave. The assumptions used in this formula are based on the linear wave theory, since we are dealing with deep water and, in such cases energy in sea waves propagates with the group velocity of the wave. This final assumption is correct mainly for narrow-banded wave fields.

3. Statistical analysis

A detailed statistical analysis has been performed, concerning the main parameters affecting the wave energy potential, by

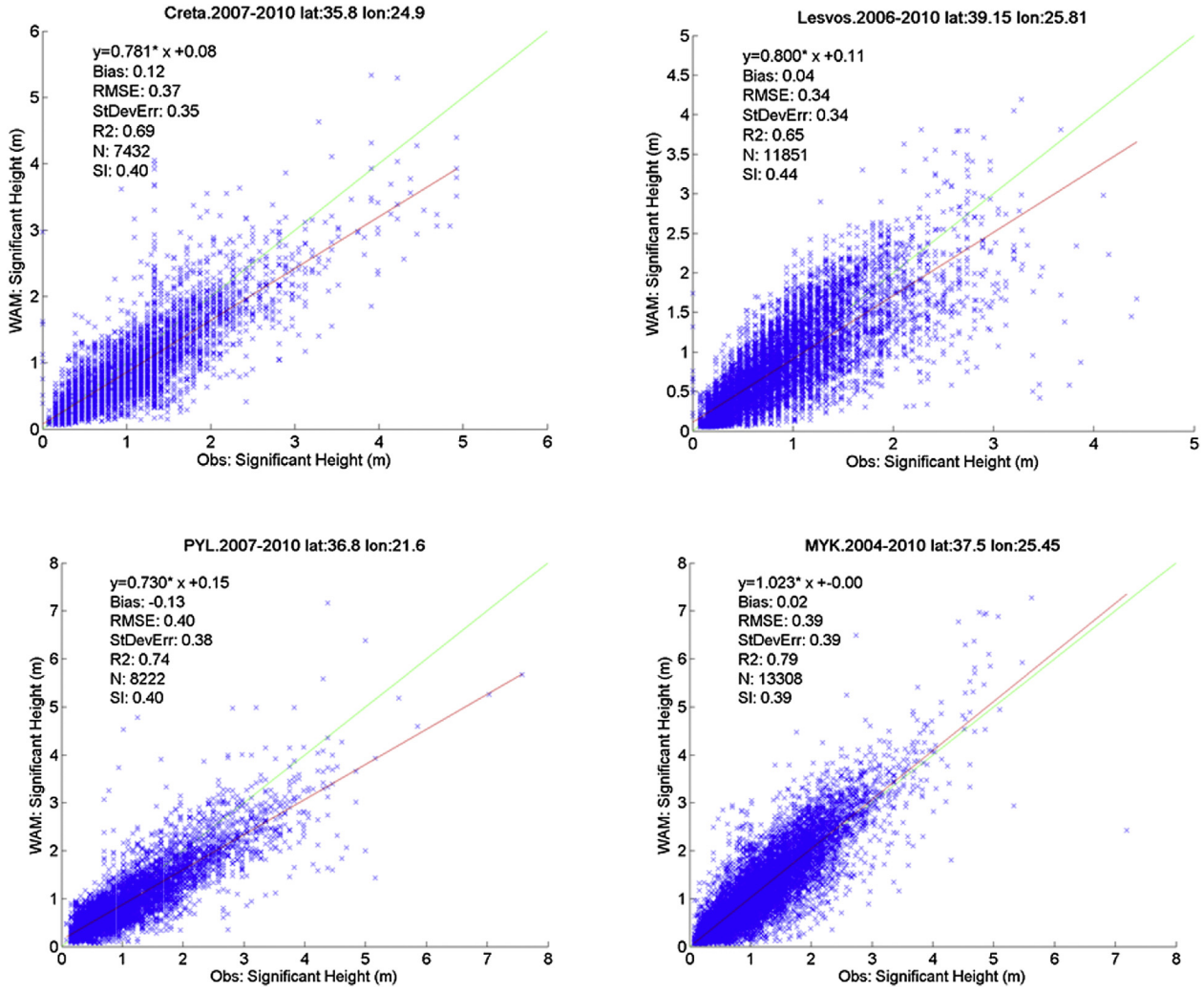

Fig. 3. Scatter plots for the 4 buoy locations and the WAM output.

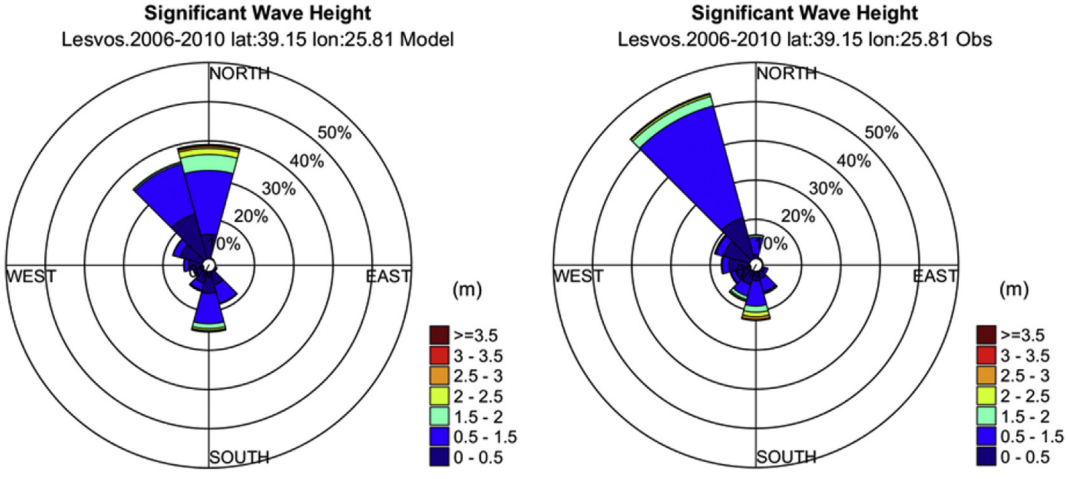

Fig. 4. Wave roses for the Lesvos buoy location: model and measurement.

utilizing statistical measures that provide qualitative information for energy applications. More precisely, the following statistical indices and measures have been used:

- The *mean value*
- *The standard deviation*
- *Skewness*:

Table 3
H_s/T_p frequency distribution for the wave model at Lesvos location.

Frequency Table:Lesvos.2006-2010 lat:39.15 lon:25.81 Model

Tp (s) \ Hs (m)	1	2	3	4
1	0	0	0	0
2	590	0	0	0
3	1601	0	0	0
4	2984	9	0	0
5	1549	512	0	0
6	454	1002	3	0
7	92	414	141	1
8	6	95	113	38
9	4	25	40	30
10	5	5	6	8
11	0	0	0	2
12	0	0	0	0
13	0	0	0	0
14	0	0	0	0
15	0	0	0	0
16	0	0	0	0
17	0	0	0	0
18	0	0	0	0
19	0	0	0	0
20	0	0	0	0

$$g_1 = \frac{\frac{1}{N}\cdot\sum_{i=1}^{N}(x(i)-\mu)^3}{\sigma^3}, \quad (4)$$

a measure of the asymmetry of the probability distribution,

- *Kurtosis*:

$$g_2 = \frac{\frac{1}{N}\cdot\sum_{i=1}^{N}(x(i)-\mu)^4}{\sigma^4} - 3, \quad (5)$$

Table 4
H_s/T_p frequency distribution for the buoy at Lesvos location.

Frequency Table:Lesvos.2006-2010 lat:39.15 lon:25.81 Obs

Tp (s) \ Hs (m)	1	2	3	4
1	0	0	0	0
2	74	0	0	0
3	1110	0	0	0
4	2155	8	0	0
5	2343	350	0	0
6	955	1078	20	0
7	264	701	193	6
8	87	152	127	22
9	16	11	29	10
10	1	0	4	0
11	0	0	0	0
12	0	0	0	0
13	0	0	0	0
14	0	0	0	0
15	0	0	0	0
16	0	0	0	0
17	0	0	0	0
18	0	0	0	0
19	0	0	0	0
20	0	1	1	0

which measures the “peakness” of the probability distribution and the impact of possible extreme values.

It should be noted that the results provided are the overall statistics, i.e., the statistics obtained by taking into account the 3-hourly values of the examined variables. This approach reveals better the detailed behavior of the examined parameters but, it may introduce noise in the statistical estimates of the variability measures. For the areas of increased interest and, in order to provide variability measures of practical value for the industry, we have included the interannual variability in Section 4.3, as it is defined in Ref. [52]: The standard deviation of the annual means normalized by the overall mean.

4. Discussion of the results

The study focused on the years 2001–2010. For this period, the results of the atmospheric model SKIRON and the sea waves model WAM were utilized. More specifically, the discussion will introduce comments concerning wind speed at 10 m and direction, significant wave height and direction, energy period and wave energy potential. In this section, the evaluation of the simulation system is included (Subsection 4.1), the analysis of the results on a 10-year, yearly and seasonal base (Subsection 4.2) and the on-site analysis for the areas with increased interest (Subsection 4.3).

4.1. Evaluation

The new version of the wave model used in the present study has been evaluated by the developing Center's (ECMWF) wave group in Refs. [7,8,38], providing detailed analysis of the performance of the model. Moreover, an application and evaluation in the North Atlantic Ocean can be found in Ref. [15], an evaluation study against remote sensing data for the Mediterranean Sea is presented in Ref. [18], while similar evaluation and analysis for the west coastline of the US (Pacific Ocean) is presented in Ref. [17].

For this work, further evaluation of the model has been performed and is presented here. The evaluation concerned the significant wave height and direction in four buoy locations, in the north and south part of Aegean Sea as well as in the south Ionian Sea (Fig. 2). The three southern buoys provide only altimetric data (i.e. significant wave height), when the northern one includes directional information as well. For this evaluation the closest grid

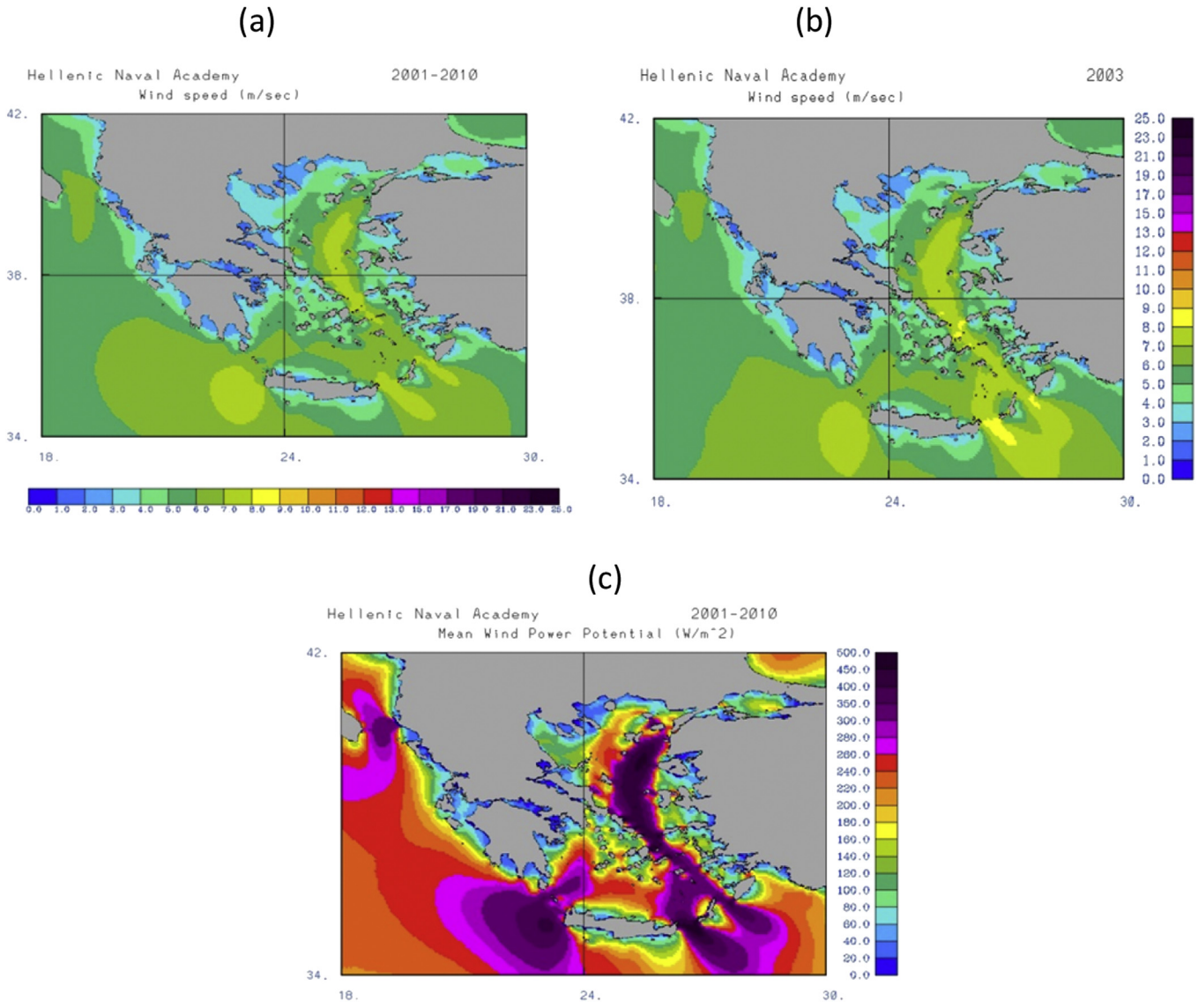

Fig. 5. 10 m Wind speed: Mean of 10 years (a) and of the year 2003 (b). Mean wind power of 10 years (c).

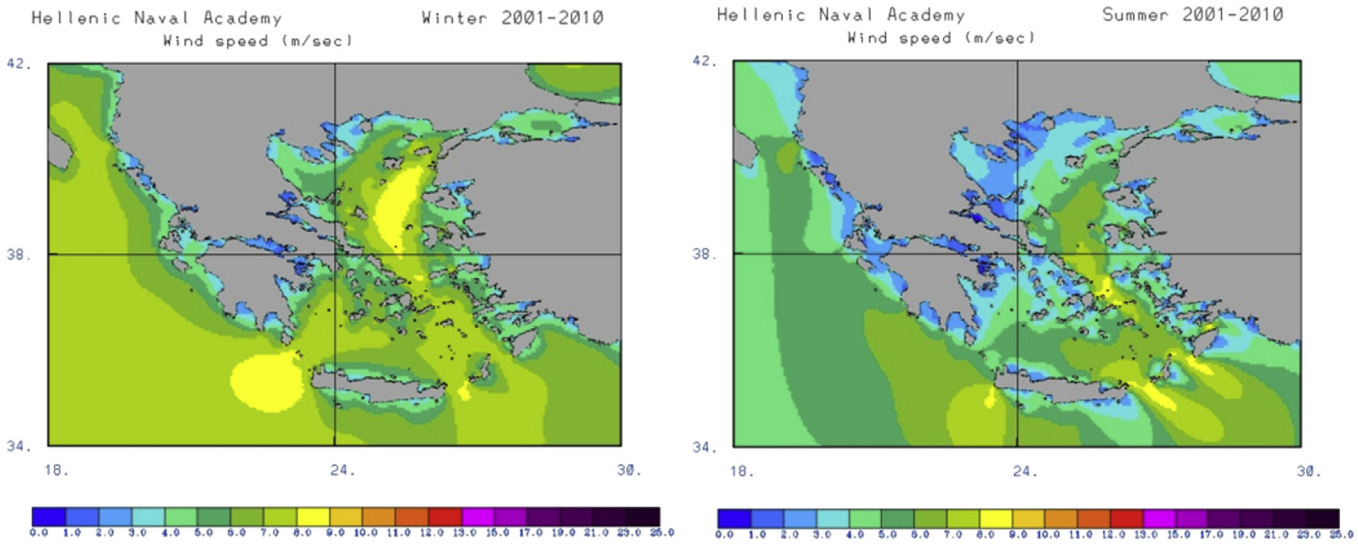

Fig. 6. Seasonal 10 m wind speed, winter and summer time.

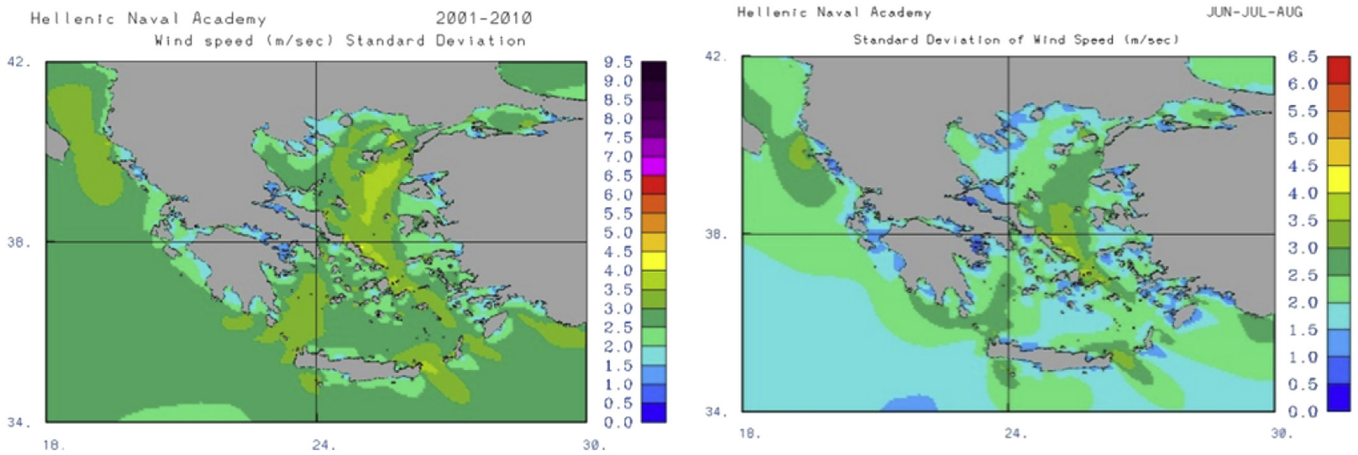

Fig. 7. Standard deviation of wind speed, 10 years and summer time.

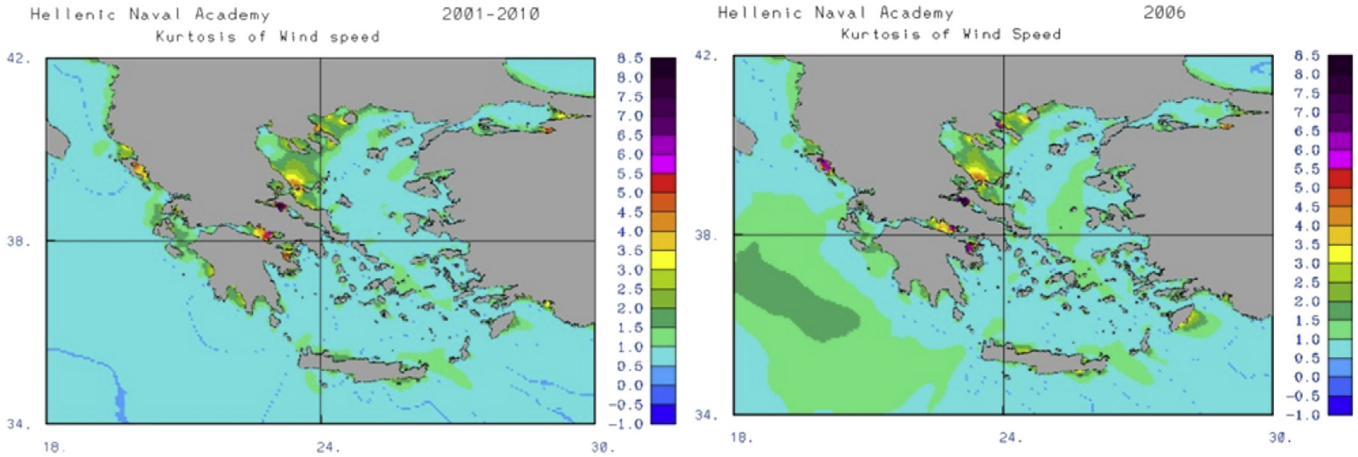

Fig. 8. Kurtosis of wind speed, 10 years and the year 2006.

point of the wave system has been used. The available period of observations for each location is included in Table 2. A light underestimation of the SWH by the model is obvious in all cases except Mykonos (Table 2 and Fig. 3). On the other hand, the direction in Lesvos is simulated efficiently, with the majority of the cases showing a north-northwestern direction of the swh, both by

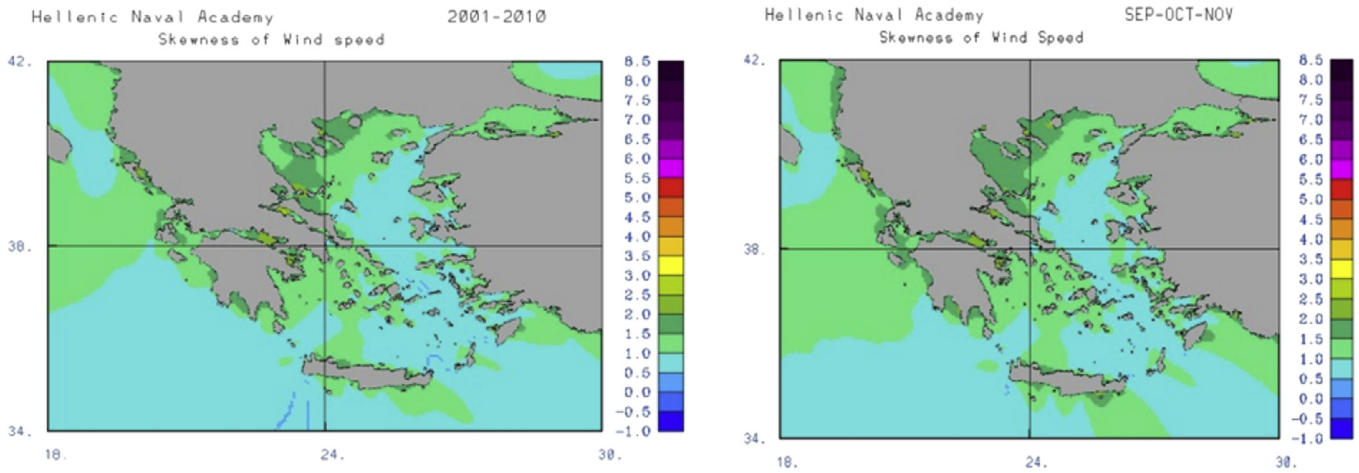

Fig. 9. Skewness of wind speed, 10 years and autumn.

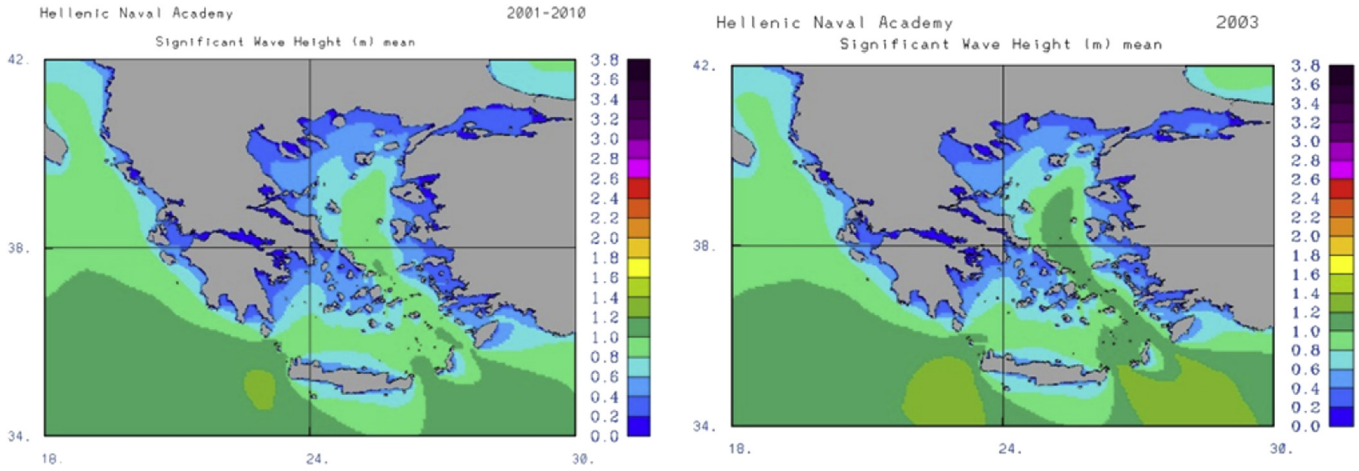

Fig. 10. Significant wave height, 10 years and the year 2003.

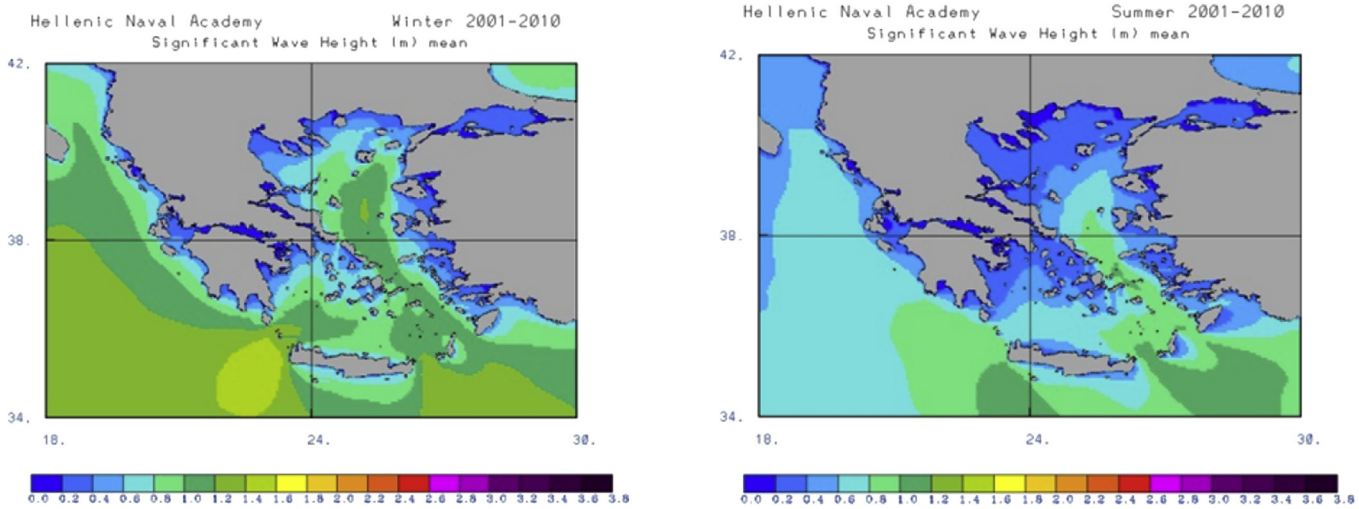

Fig. 11. Seasonal significant wave height, winter and summer time.

model and observations (Fig. 4). The most frequent SWH range is between 0 and 2 m, as shown in the H_s/T_p distribution diagrams (Tables 3 and 4). These results show the good distribution agreement between model and observations and are of increased importance because of the role of such tables in the choice of the proper location for the wave power generators. In this area, the

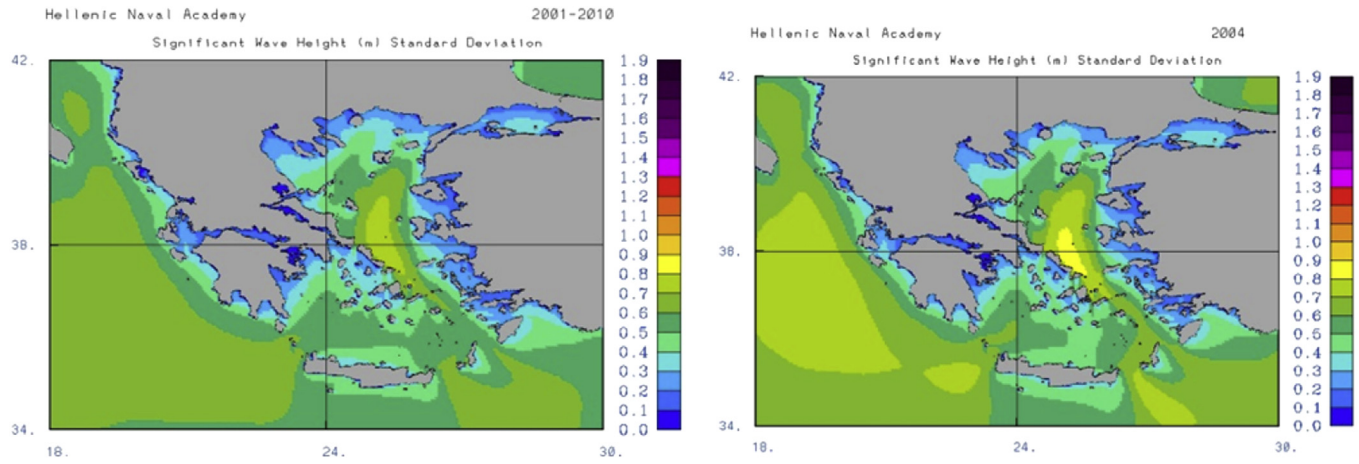

Fig. 12. Standard deviation of significant wave height, 10 years and the year 2004.

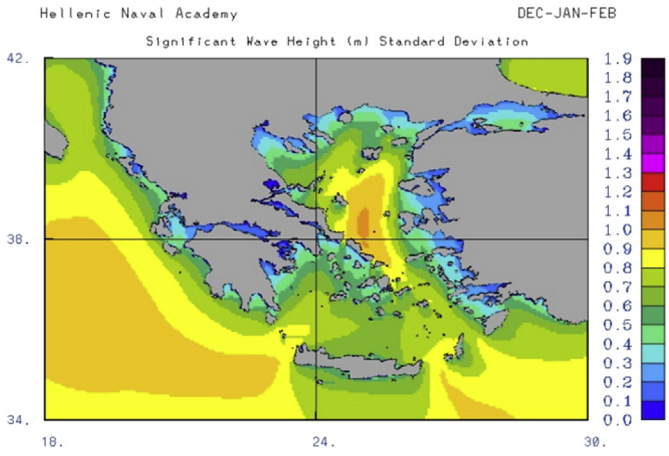

Fig. 13. Standard deviation of significant wave height, winter time.

scatter plots (Fig. 3) show also good agreement between WAM and buoy measurements.

4.2. Temporal analysis

The above described study focused in the main meteorological and wave parameters affecting the wave energy potential. An analysis on a 10-years, year-by-year and seasonal base has been performed, concerning all the statistical indices utilized (Mean, standard deviation, skewness and kurtosis) for the wave energy potential and the main atmospheric (wind) and sea wave parameters (significant wave height, direction and mean wave period) affecting it. We have to note here that the basic maps are presented, as well as a choice of the most characteristic ones for each parameter, from the annual and seasonal study.

The study of wind speed shows maximum intensities over the areas west and east of Crete and in a tunnel crossing the eastern side of Aegean Sea, with intensity up to 8 m/sec (Fig. 5a). We should note that the color scale bars are the same for the maps of each parameter in order to be comparable with each other. The same pattern is valid for the wind power, since it is depended on wind speed only (Fig. 5c). Wind speed is more intense during the winter, as expected (Fig. 6). This is due to the general atmospheric circulation at this period of the year, with several low pressure systems crossing over Balkans. This pressure gradient results to high wind speeds. The next season with increased values is summer, because of the etesian winds prevailing over Aegean Sea, mainly in August. As far as the yearly stats concerned, wind speed increased its intensity over the same areas depicted by the 10 year study. We should remark that Cyclades islands are playing the role of an obstacle to the wind (and the waves) propagation.

The northern parts of Greek seas (northeastern Aegean Sea) show high values of standard deviation (4 m/sec), which means

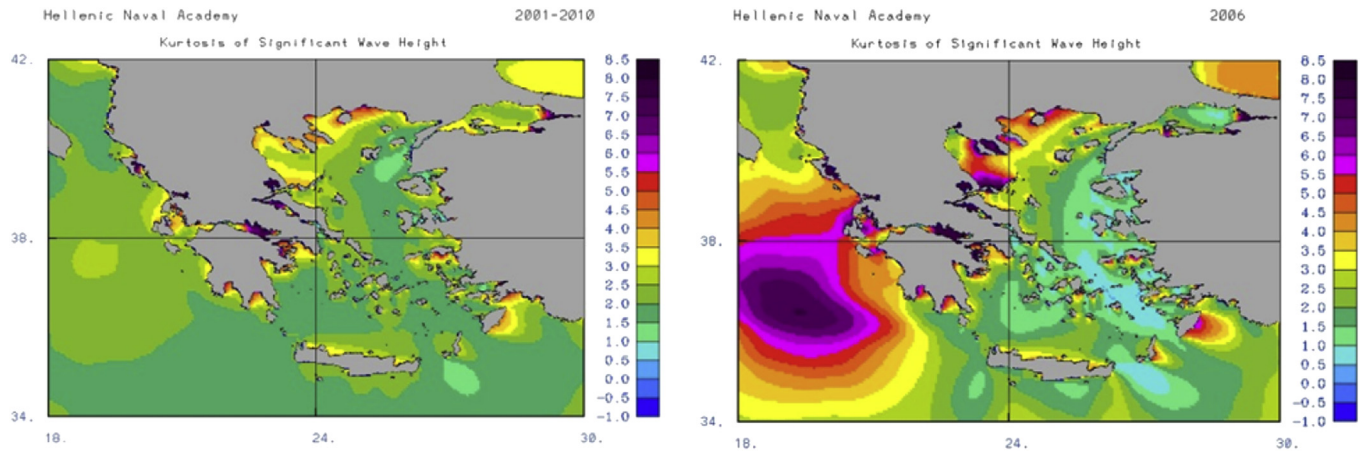

Fig. 14. Kurtosis of significant wave height, 10 years and the year 2006.

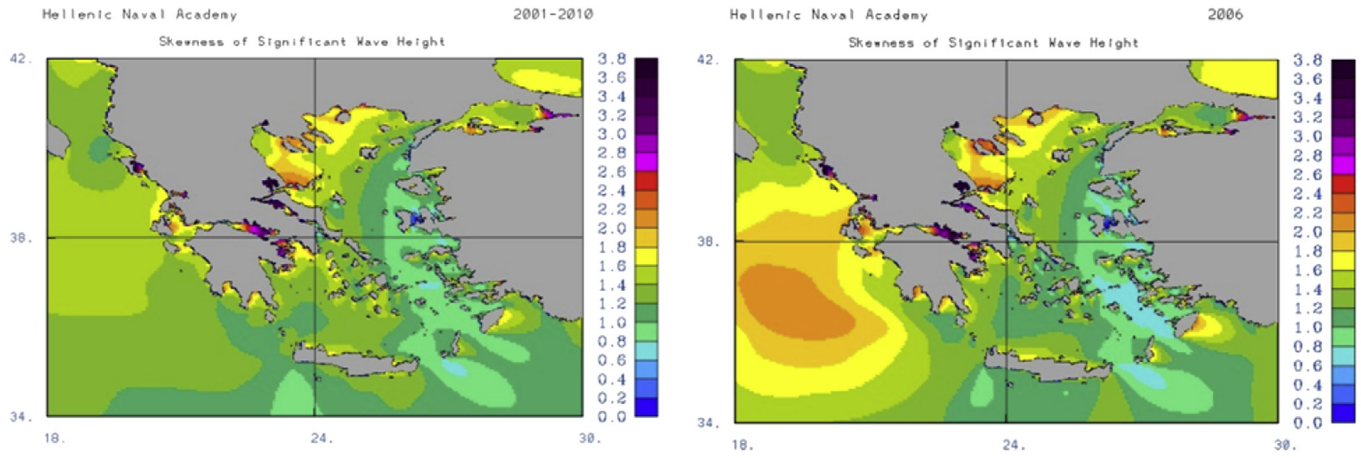

Fig. 15. Skewness of significant wave height, 10 years and the year 2006.

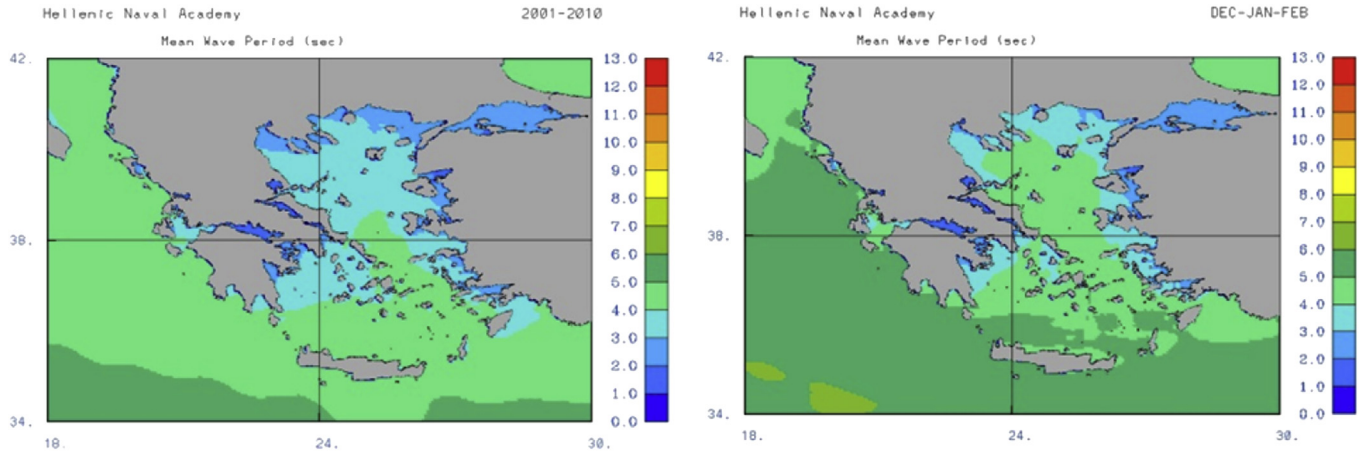

Fig. 16. Energy wave period, 10 years and winter time.

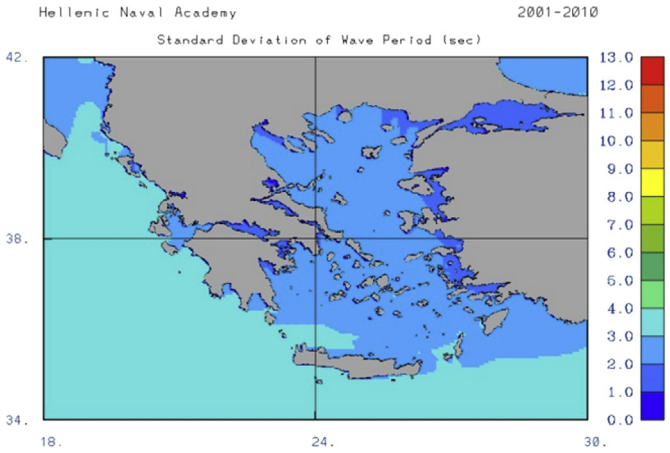

Fig. 17. Standard deviation of the energy wave period, 10 years.

that the wind speed in these parts is of high variability. Standard deviation is higher during winter, but is quite small during summer time (Fig. 7). The mean and the standard deviation of wind speed are having an almost constant yearly behavior.

Coastal areas reveal high kurtosis values, meaning that the distribution of wind speed is more affected, in these areas, by high values (Fig. 8). Skewness, as kurtosis, is also considerable near coastal areas, with higher values during summer (Fig. 9), when the weather is mild and any extreme event may play an important role. This result leads to the conclusion that there is a move of the distribution towards higher wind intensities.

No long term variations are existing in the yearly study of wind speed in this decade. Yearly skewness is being also maximized in the central Ionian Sea and in the south parts of Thermaikos Gulf (not shown here). This is a fact that may be attributed to the atmospheric and wave models: in those closed gulfs (like Thermaikos), the resolution used cannot simulate accurately the local phenomena because of the small number of grid points in these sea areas. The same conclusions for the coastal areas and Thermaikos Gulf stand for the Kurtosis values (Fig. 8). Moreover, it should be noted that in areas with low mean values, any significant weather event may play an important role in the general situation described. Finally, there is a rather symmetric and low risk wind speed distribution (and significant wave height, as will be shown in Fig. 14) over the areas with increased mean values.

Significant Wave Height (SWH), which is a main factor in the calculation of wave energy potential, is having its higher mean values (1.2–1.4 m) in the south seas (South Ionian Sea, South Cretan Sea) and this fact may be attributed to swell coming from south and central parts of Mediterranean (Fig. 10). The higher values are shown in the winter time (1.6 m) and then during spring (Fig. 11).

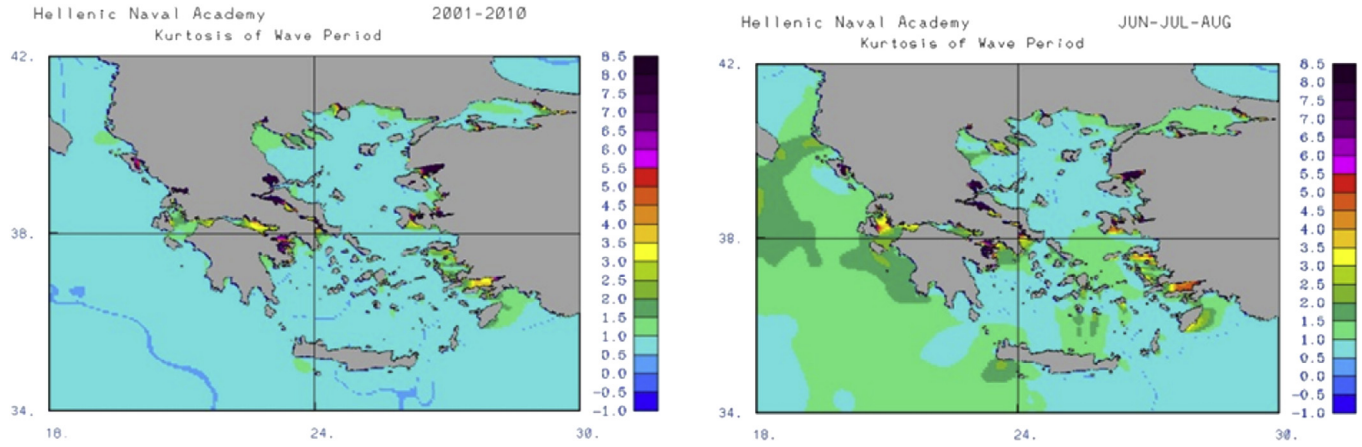

Fig. 18. Kurtosis of the energy wave period, 10 years and summer time.

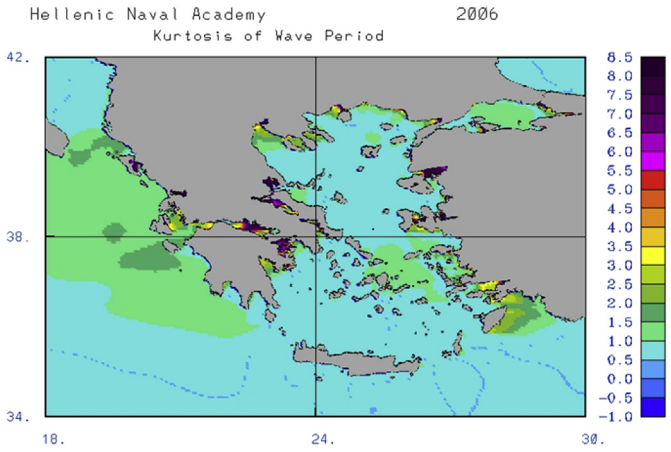

Fig. 19. Kurtosis of the energy wave period, the year 2006.

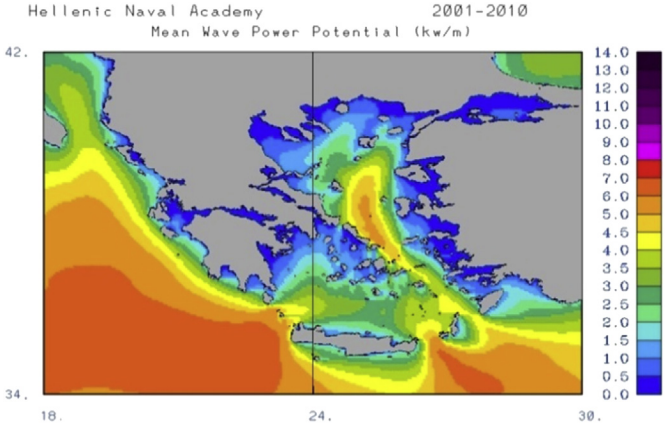

Fig. 21. Mean wave power potential, 10 years.

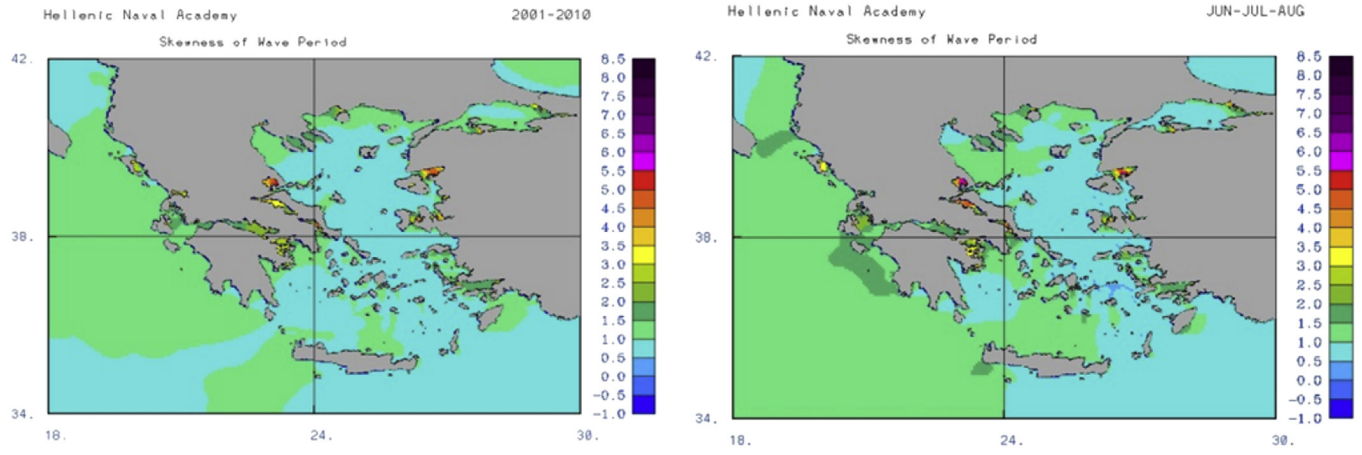

Fig. 20. Skewness of the energy wave period, 10 years and summer time.

Similar results were accumulated by Ref. [24]; who studied the wave power potential in Aegean Sea with input by the ERA Interim data. This seasonal pattern agrees with the wind pattern during winter, when the increased wind speeds play an important role to the waves as well. The areas of interest during winter remain to be the tunnel in the east Aegean, the south sea parts (as also described for the wind speed) and Ionian Sea. In summer, the wind waves are not capable of keeping high SWH for long periods. This time of the year, we have increased wind waves with low mean wave period. This results, as we will see in Fig. 23, to decreased values of wave power potential. In the Ionian Sea, there are increased mean values and decreased uncertainty.

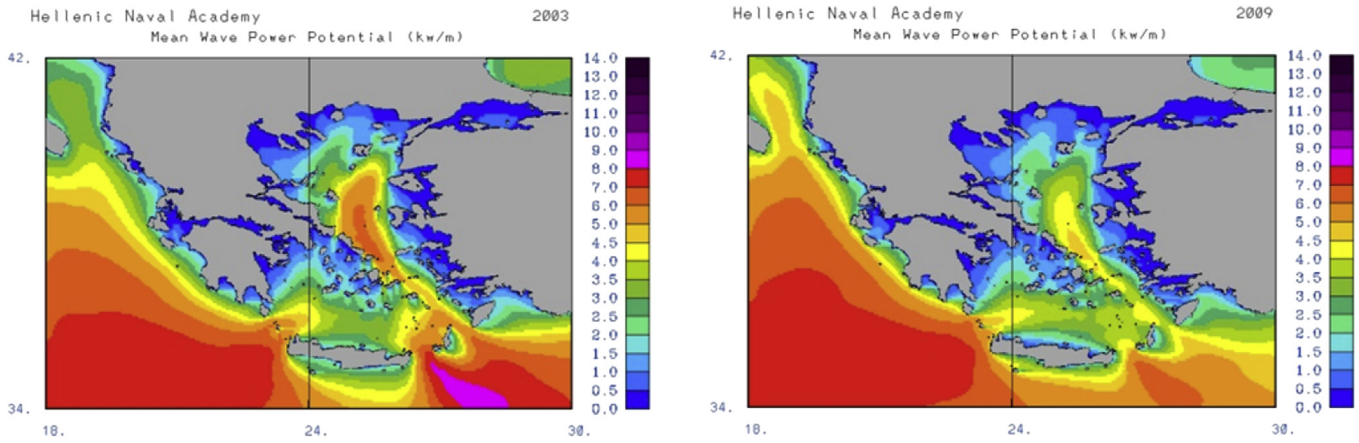

Fig. 22. Mean wave power potential, the years 2003 and 2009.

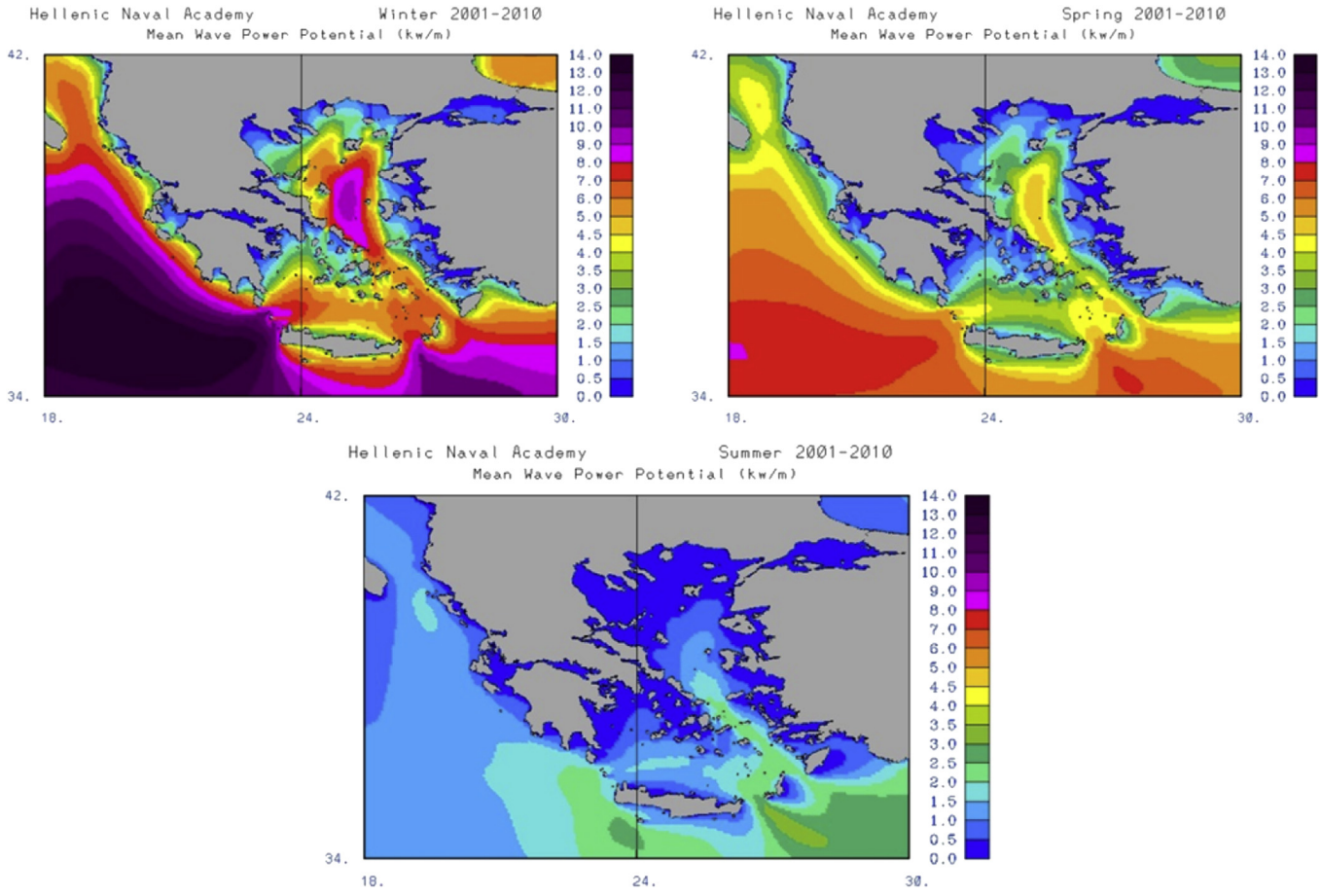

Fig. 23. Seasonal mean wave power potential, winter, spring and summer.

In a yearly basis, the area with the higher SWH (1.4 m) is constantly the one west of Crete, with the eastern part following (Fig. 10). The open Ionian Sea as well as the tunnel in the eastern parts of Aegean are also the areas with high interest. On the other hand, there are no significant differences from year to year.

The terrain of the Cyclades islands which is reducing the wind speed, is not allowing to the swell to cross the area of central Aegean, neither from south to north nor the opposite. This creates the shadow effect on the back side of the islands. The same conclusion also stands for Crete.

The standard deviation increases in similar to the wind speed max areas (Fig. 12). This is due to the fact that the wind waves vary according to the weather conditions of the relevant time period. The northern part of the eastern Aegean tunnel is the area with high deviation values (up to 0.9 m) (Fig. 13).

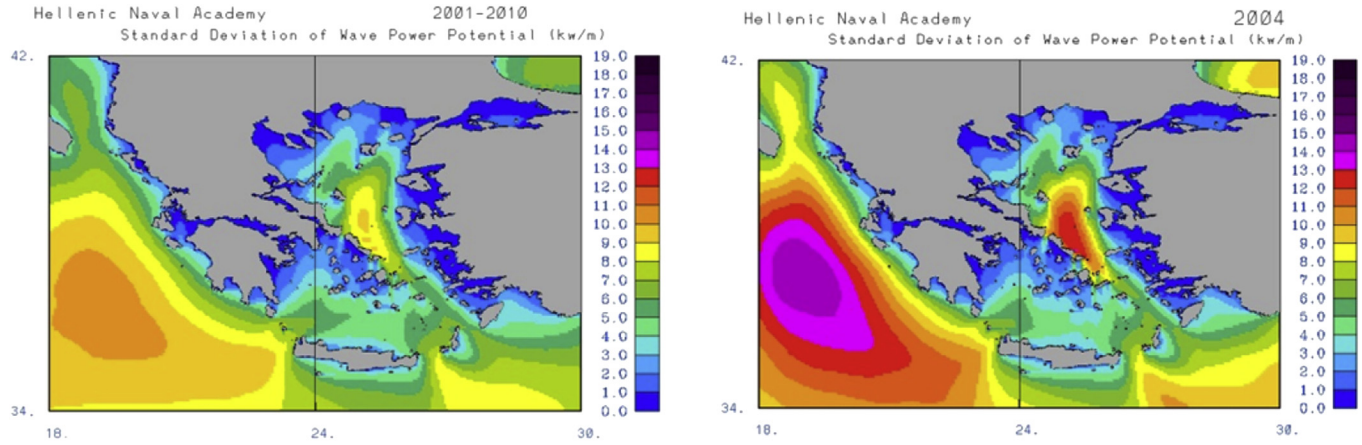

Fig. 24. Standard deviation of the wave power potential, 10 years and the year 2004.

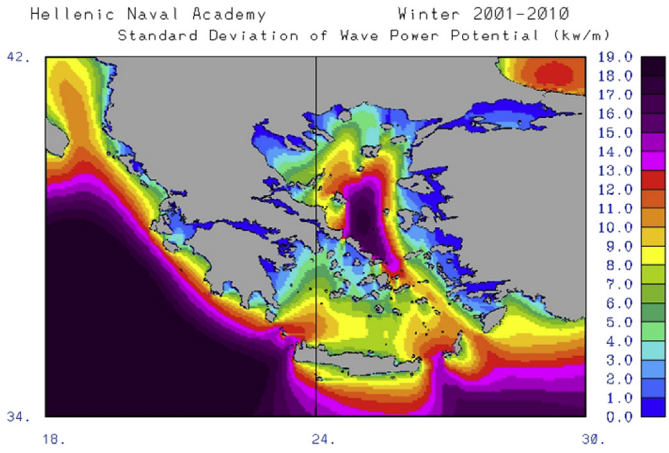

Fig. 25. Standard deviation of the wave power potential, winter time.

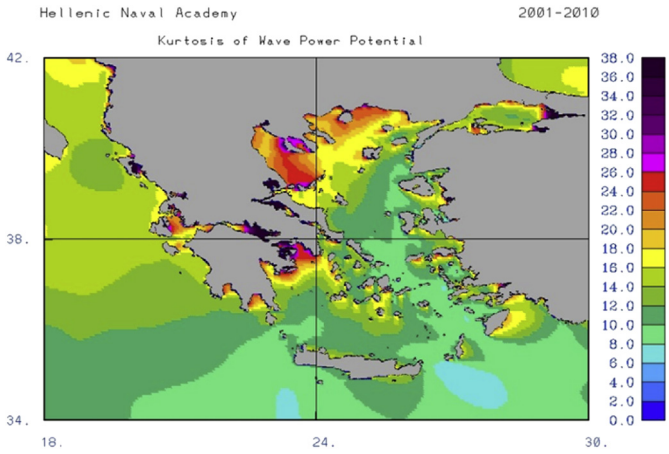

Fig. 26. Kurtosis of the wave power potential, 10 years.

Kurtosis is growing near the coasts and in the Ionian Sea, mainly its central parts (Fig. 14). This shows that in these areas the distribution of swh tends to depend more on high values of SWH. The variability from year to year is considerable. So, one may expect different non-frequent value distribution and impact.

Skewness is maximizing near the coasts, in the central Ionian Sea and in the south parts of Thermaikos Gulf (Fig. 15). The variability from year to year is smaller than the one in kurtosis.

The energy wave period is mainly depended on the swell part of the waves, though taking bigger values (6 s) at the southern parts (Fig. 16). The standard deviation of the wave period is almost constant within the decade (as shown representatively in Fig. 17). The skewness and the kurtosis are showing considerable values in the closed gulfs (Figs. 18–20), where the period is having low values with the problem of the wave model simulation (as described earlier) in those closed areas adding in those variations.

The Wave Power Potential gives increased values (6–7 kW/m) in the same areas with SWH, but also in a major area of Ionian Sea (Fig. 21). This fact may be attributed to the significant values of SWH, as well as of the wave period prevailing in these areas. At the same time, the wind power is increased over these areas (Fig. 5c), leading to the conclusion that a combined exploitation of these two different atmospheric phenomena could give better and more stable results in the renewable energy exploitation.

The favor year for the mean wave power potential was 2003 with values, east of Crete, reaching 9 kW/m and interesting areas, those of southwest parts and the tunnel of eastern Aegean (Fig. 22). Compared to the results of Jadidoleslam et al. [24]; slightly greater values are presented here due to better model domain setup and resolution, which allows swell waves reach parts of the study area.

Those are the areas of increased interest for the whole decade with the maximum from year to year varying from 7 to 9 kW/m. The most interesting seasons are winter and spring (Fig. 23). Significant yearly variation exists in mean wave power values as well as in the corresponding deviation values, as shown in the two representative maps of Fig. 22. However, the deviation is quite important in the open Ionian Sea and especially the southwestern parts (Figs. 24–25) with values in year 2004 up to 15 kW/m.

Significant high values are evident for the kurtosis, with lower in the south part areas (Figs. 26–27). Kurtosis is growing near the coasts and in the Ionian Sea, mainly its central parts. This shows the increased impact of extremes for wave power over the Ionian Sea and the wind-wave areas of Aegean Sea.

Skewness is having low values in the eastern Aegean tunnel and shows variability in the other open sea areas (Fig. 28). Nevertheless, it keeps high values in the coastal areas, showing divergence from a normal-symmetric distribution of the wave power potential around the mean value. Similar conclusions may be extracted for the swell dominated areas of the western seas.

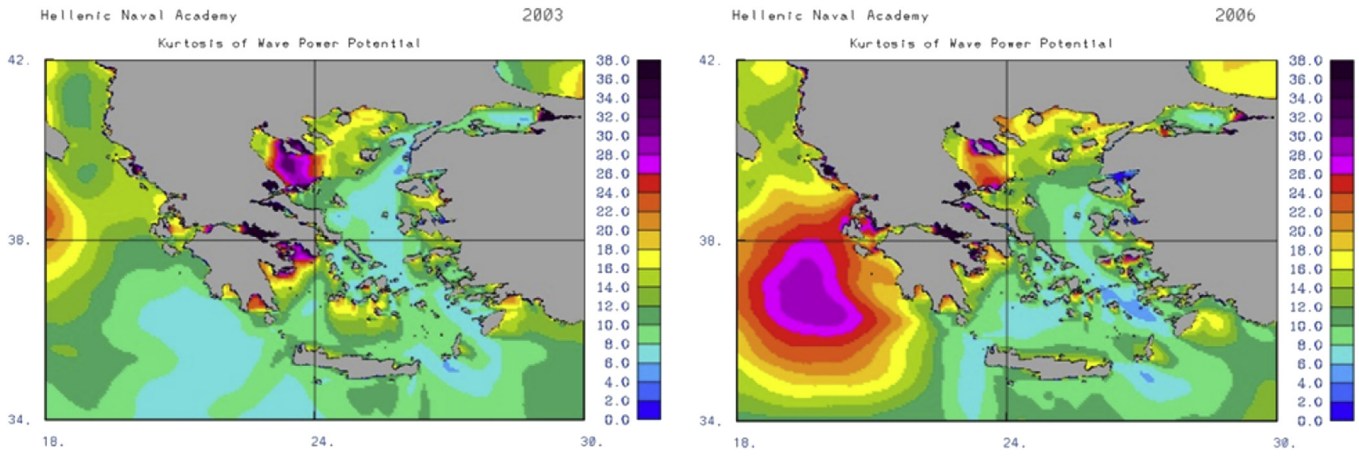

Fig. 27. Kurtosis of the wave power potential, the years 2003 and 2006.

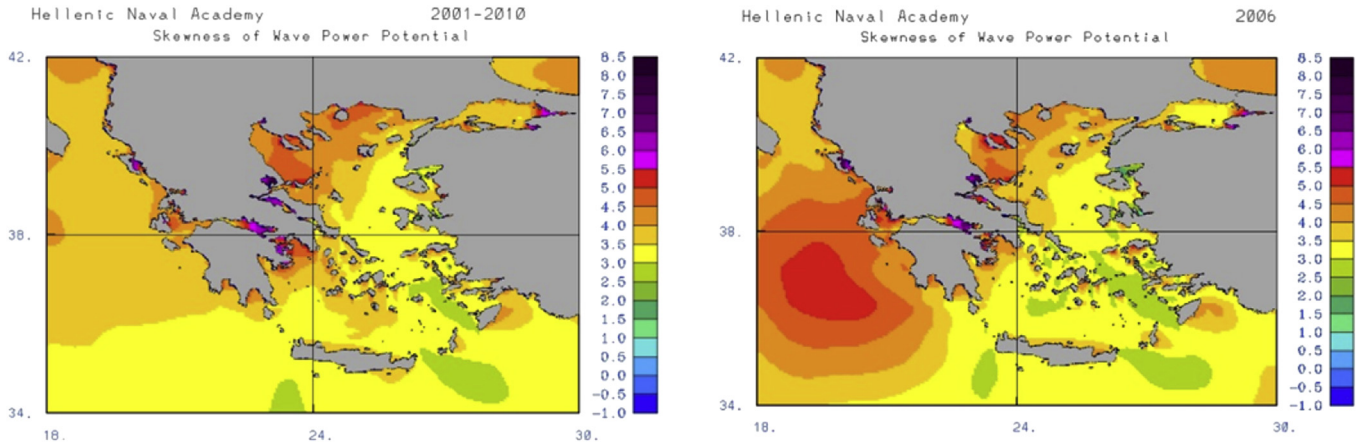

Fig. 28. Skewness of the wave power potential, 10 years and the year 2006.

4.3. Site analysis

In the next table (Table 5), we present the interannual variability (as described in Section 3 and defined in Ref. [52]) of the parameters examined in four points of increased interest, which are shown in Fig. 29. We note that in these areas, there is a slight variation from year to year. The wave energy potential is relevantly stable because of the long wave periods prevailing there.

A study for the main wind and wave directions, as well as the distribution of wind speed at 10 m, SWH and mean wave period, prevailing in two points (point 1 and 2 in Fig. 29) of increased interest for energy applications is also presented.

The prevailing wind directions over the northern Aegean Sea (point 1 in the map) is the north and northeast with the south-southeast following (Fig. 30). The same time, sea waves are having the same pattern, but the straight south direction is existing without the southeast one. This difference shows that the south waves in this area are having a swell component.

For the same point, the values of 10 m wind speed show a wide distribution, with the Weibull fitting better and the majority of the values being between 3 and 10 m/sec (Fig. 31). The 95% of the distribution (which is an extreme value indicator) is included with

Table 5
Interannual variability for the 4 points presented in Fig. 29 (below).

Interannual variability	Point 1	Point 2	Point 3	Point 4
Wind speed	0.04	0.01	0.04	0.07
Significant wave height	0.10	0.06	0.06	0.10
Energy period	0.04	0.05	0.02	0.01
Wave energy potential	0.20	0.12	0.14	0.16

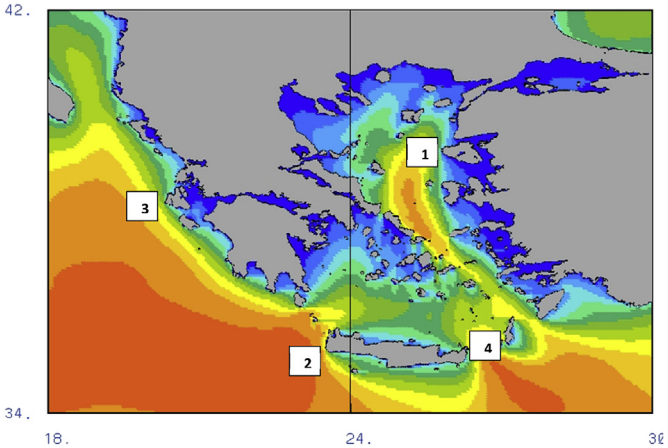

Fig. 29. Wind and wave roses: areas of study.

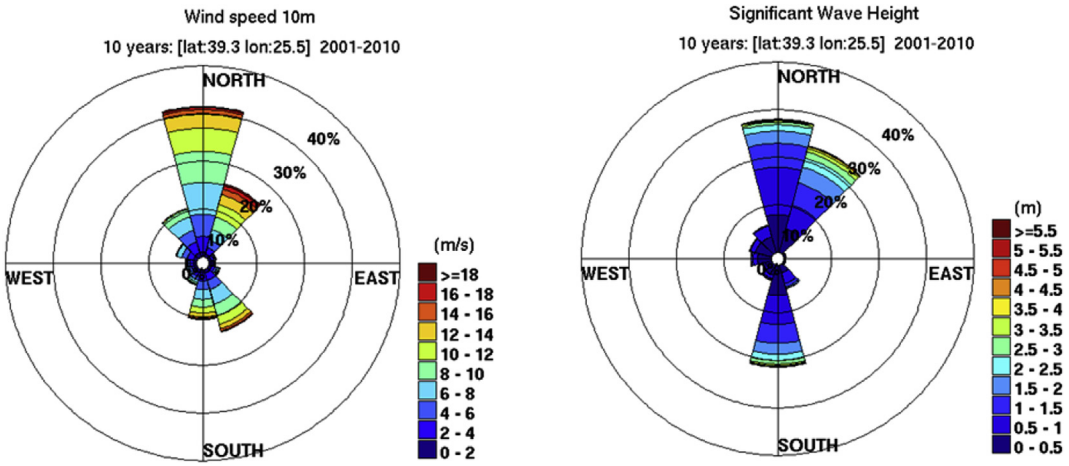

Fig. 30. Wind and wave roses for area 1 (Northern Aegean Sea, west of Mytilini island).

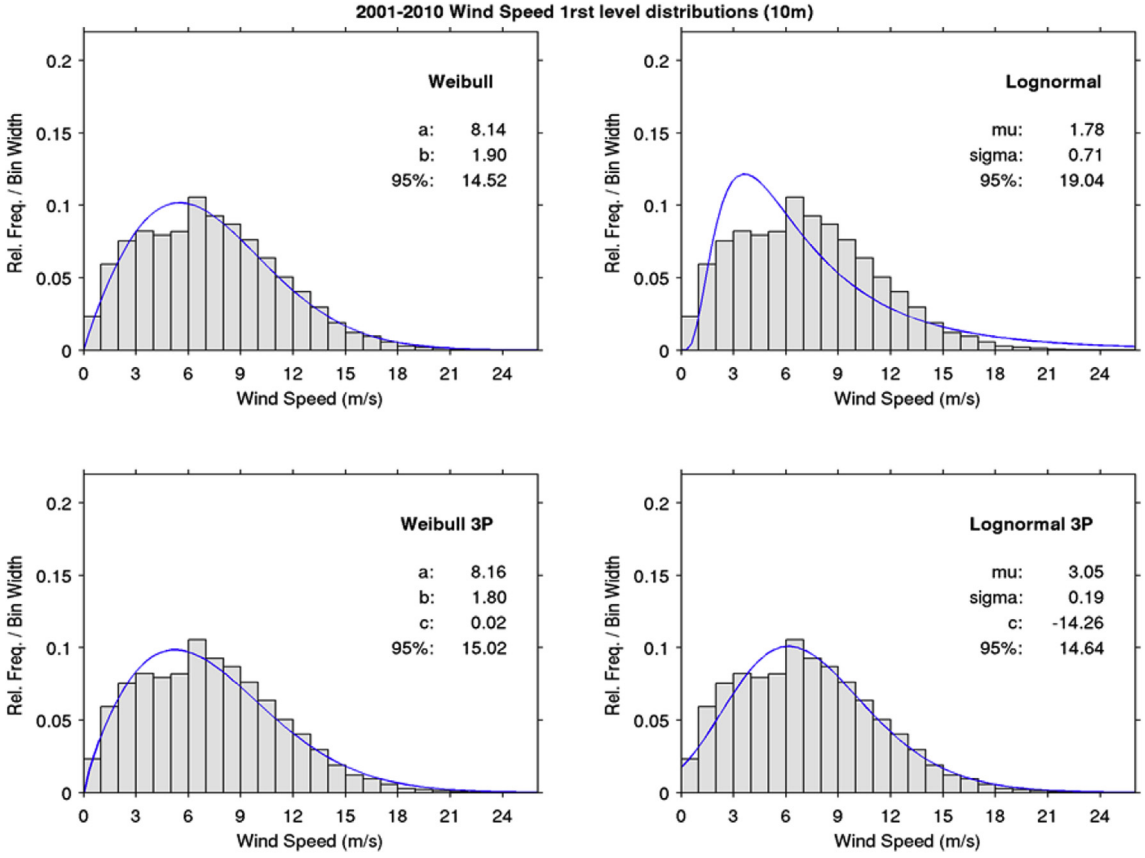

Fig. 31. Wind speed (10 m) distribution for area 1 (Northern Aegean Sea, west of Mytilini island).

wind speeds less than 15 m/sec.

Different distribution is valid for the SWH (Fig. 32), with the Weibull describing best this parameter again, but with different shape and scale parameters. The SWH values are included in a 95 percentile less than 2.5 m and the distribution is skewed to low values.

The energy wave period at the same time is mainly concentrated between 3 and 5 s, with the lognormal profile fitting better to the description of this parameter (Fig. 33). The 95 percentile of the relevant values is approximately 6 s. The relevant significant wave height (Hs) and energy period (Te) distribution, which is important information that comes out from the wave energy assessment is presented in Table 6.

The study of the area west of Crete (point 2 in the map), which is of great interest because of the increased availability of wave power potential, shows winds blowing from all the northwest directions (270–360°), when the waves are focused in the main northwest direction (300°) as well as the north one (360°) (Fig. 34). Here, a

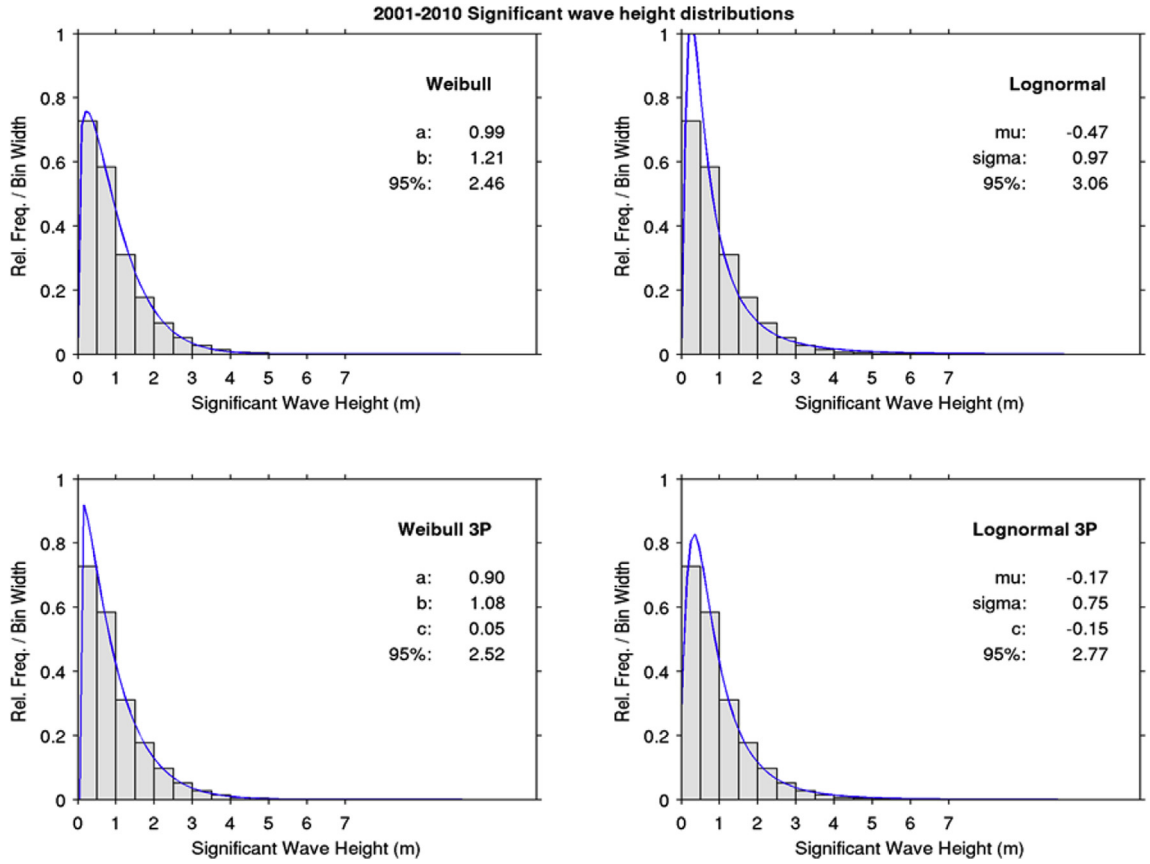

Fig. 32. SWH distribution for area 1 (Northern Aegean Sea, west of Mytilini island).

combination of the wind and the swell components is contributing to the existence of these two main wave directions.

It is important to notice at this point that the increased standard deviation values lead to elevated index of variation values. This is, however, mainly a result of the very low mean values of the parameters under study. So, the variability of the data is not, in fact, that high in absolute values and the estimations provided are not that high risky. Towards the better understanding of the analysis proposed, the discussion based on asymmetry and kurtosis values of the results is also helpful revealing possible increased impact of extreme values to the data under study.

For this area, the values of 10 m wind speed show a less skewed (compared to point 1) distribution (Fig. 35), with the Lognormal 3P fitting better, and the majority of the values fluctuates between 4 and 10 m/sec. The 95% of the distribution (which is an extreme value indicator) is included with wind speeds less than 12.5 m/sec.

The same distribution (the Lognormal 3P) with wind speed fits better for the SWH as well, but with totally different shape and scale parameters (Fig. 36). The SWH values are in a 95 percentile less than 2.7 m and the distribution is skewed to low values.

The energy wave period at the same time is mainly concentrated within a range between 3 and 6 s, with the lognormal 3P profile fitting better to the description of this parameter (Fig. 37). The 95 percentile of the relevant values is approximately 7.5 s. These stats show that the shape and scale parameters are area sensitive, when we compare to the previous point. The Hs/Te diagram (Table 7), compared to the one of Lesvos island, is showing a move of the values to higher energy periods and significant wave heights. This reconfirms that in the south areas, swell is playing an important role to the relevant parameters.

5. Conclusions

The mapping of the wave energy potential over Eastern Mediterranean Sea and especially the greater Greek area is the subject of this study. We have explored the corresponding spatial and temporal distribution of the atmospheric and sea wave parameters affecting the wave energy. The numerical models used for the simulation of the atmospheric and sea state parameters, have been employed for a 10 year period (2001–2010) at a resolution of 0.05°. The system was run in a hindcast mode, exploiting any available observational data (by satellites and meteorological stations) by data assimilation techniques, leading to improved analysis results. The relevant outputs have been analyzed by the use of a variety of statistical measures, monitoring the mean values, the variation, the asymmetry and the potential impact of extreme/non-frequent values.

The main conclusion is that the Greek sea area encloses interesting points for exploitation of wind and wave energy potential. More specifically:

- Atmospheric and wave models can simulate accurately the weather conditions in these areas with the proper configuration, as revealed by the evaluation procedure.
- The primary areas of interest for wind are the Aegean Sea tunnel and the areas west and east of Crete. There is no significant variation from year to year. Seasonally speaking, winter is the most interesting period, as expected. The dependence on high values is important in some, mainly coastal, areas.

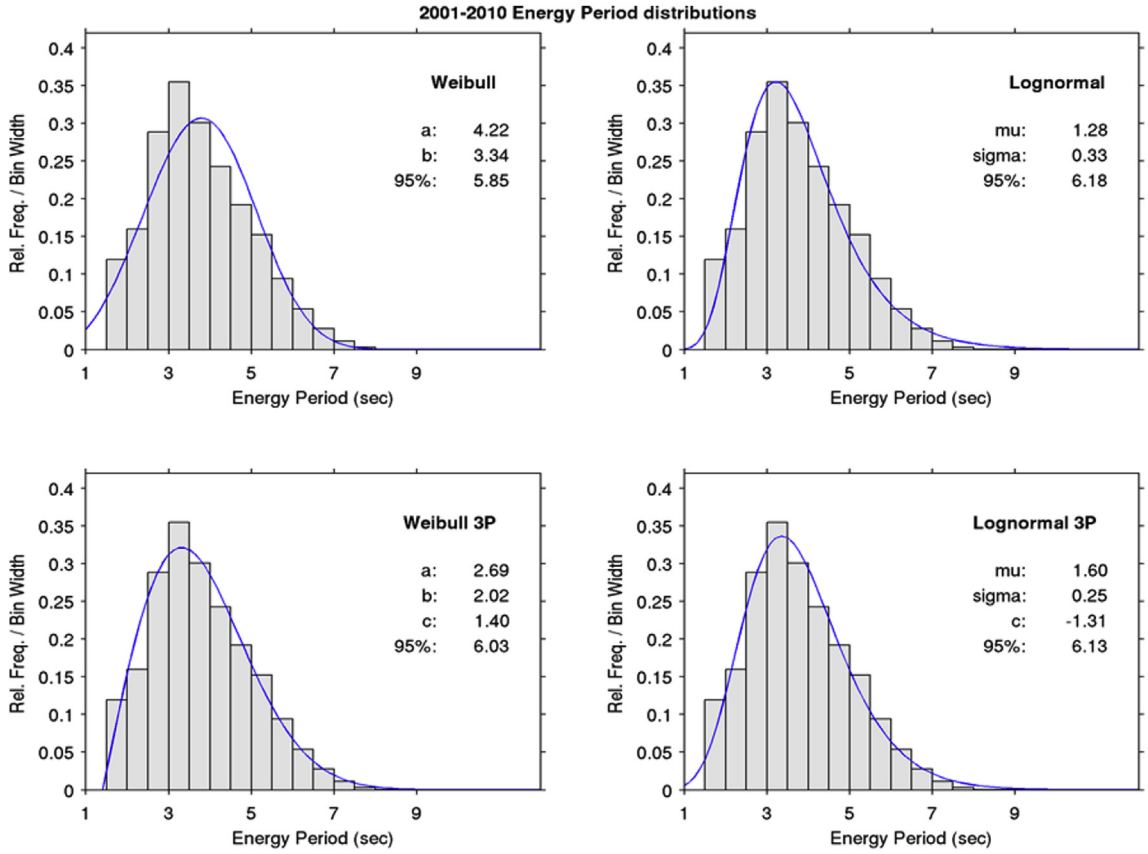

Fig. 33. Energy wave period distribution for area 1 (Northern Aegean Sea, west of Mytilini island).

Table 6
H_s/T_e frequency distribution (model) for the Lesvos location.

10 years: [lat:39.3 lon:25.5] 2001-2010

Te (s) \ Hs (m)	1	2	3	4	5	6	7	8	9	10	11	12
1	0	0	0	0	0	0	0	0	0	0	0	0
2	5189	0	0	0	0	0	0	0	0	0	0	0
3	19683	1	0	0	0	0	0	0	0	0	0	0
4	27166	1158	0	0	0	0	0	0	0	0	0	0
5	4576	14464	29	0	0	0	0	0	0	0	0	0
6	420	5809	4927	9	0	0	0	0	0	0	0	0
7	19	227	1592	1630	96	0	0	0	0	0	0	0
8	0	9	44	168	318	70	6	0	0	0	0	0
9	0	0	3	4	17	9	3	0	0	0	0	0
10	0	0	0	0	0	1	1	0	0	0	0	0
11	0	0	0	0	0	0	0	0	0	0	0	0
12	0	0	0	0	0	0	0	0	0	0	0	0

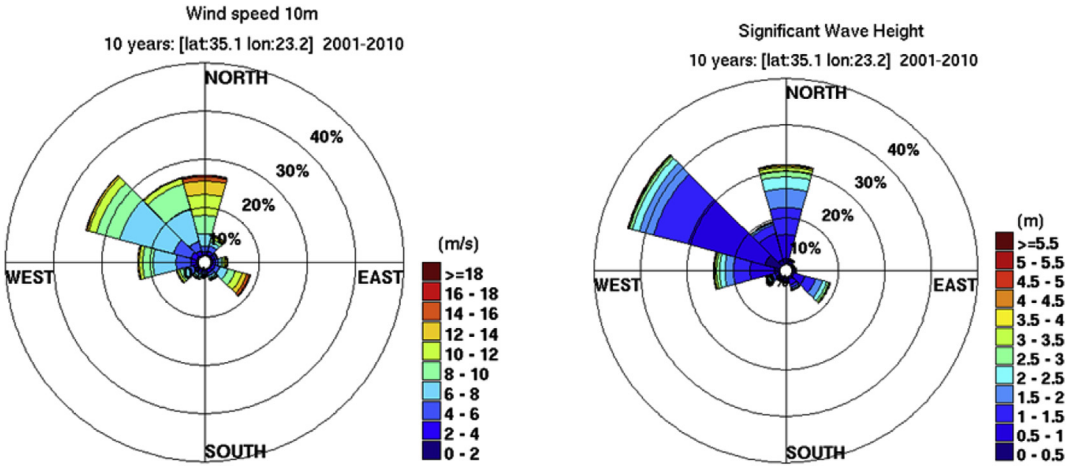

Fig. 34. Wind and wave roses for area 2 (West of Crete).

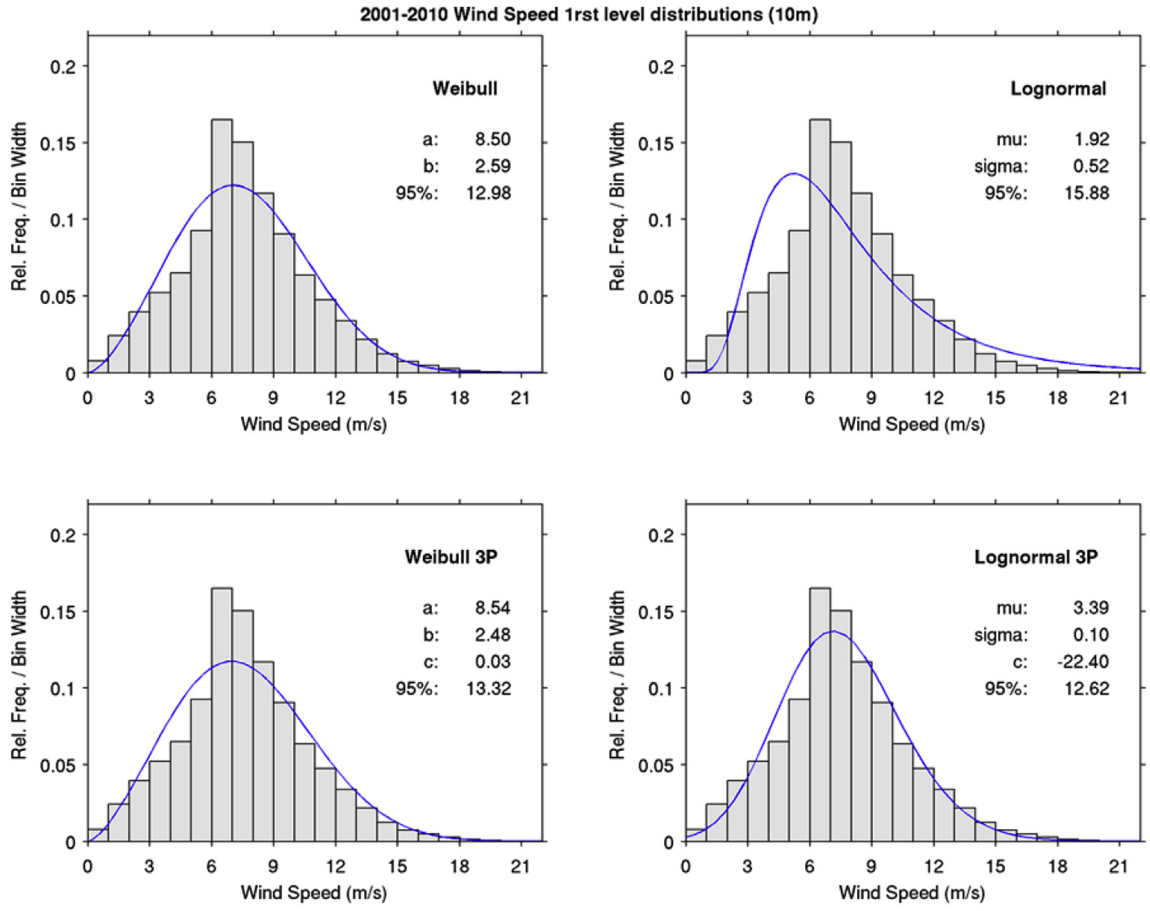

Fig. 35. Wind speed (10 m) distribution for area 2 (West of Crete).

- For the waves, primary role is having the swell dominated areas, so higher significant wave height values exist in the southwest parts. Winter is the season with increased wave heights.
- Islands are playing a role of an “umbrella” in the propagation of the waves (shadow effect).
- The most energetic offshore areas of the Greek basin, in a wave energy potential point of view, are the southwestern parts (Ionian and west part of Cretan Seas), with mean wave energy potential of about 7 kW/m. The wave power potential in these areas is more stable, because of the long wave periods prevailing there.
- The dependence on extreme weather events, as well as the distribution of each parameter affects the energy potential, especially in the closed gulfs and the northern parts of the area under study. This is proved by the elevated positive kurtosis values.

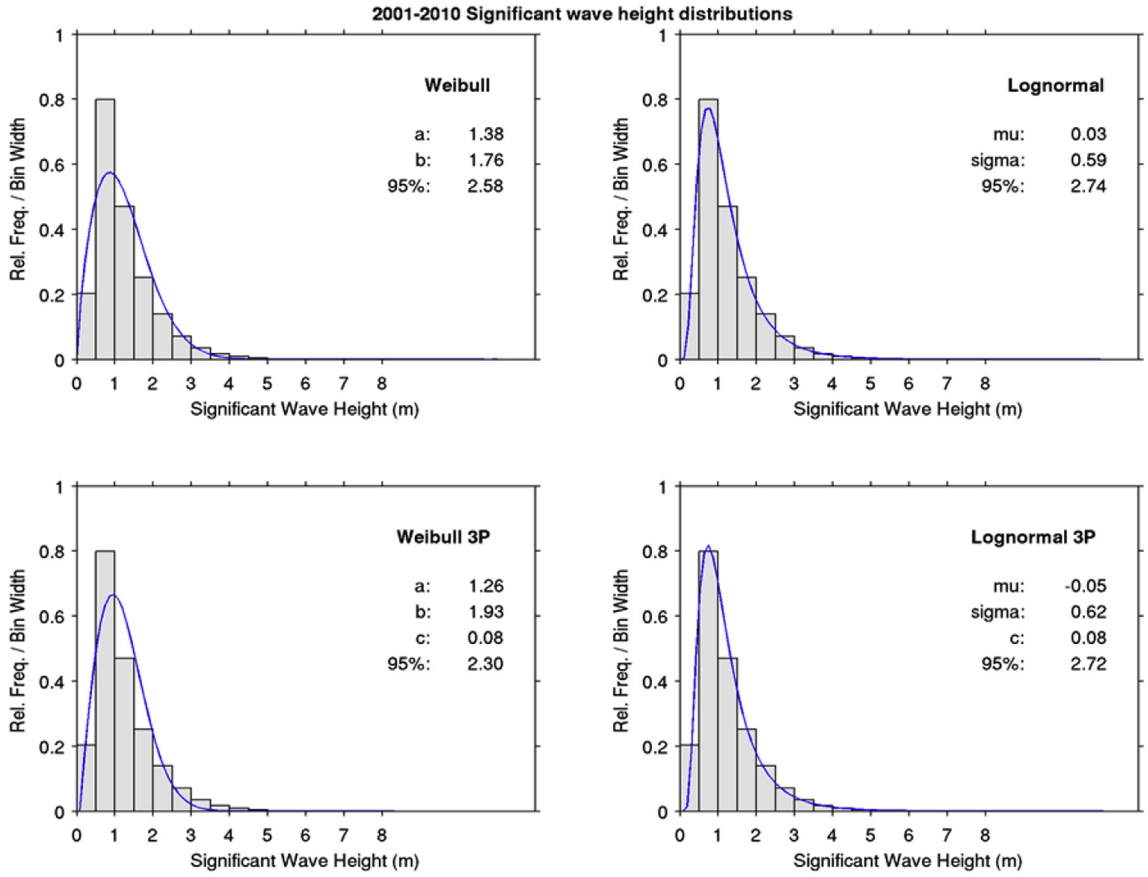

Fig. 36. SWH distribution for area 2 (West of Crete).

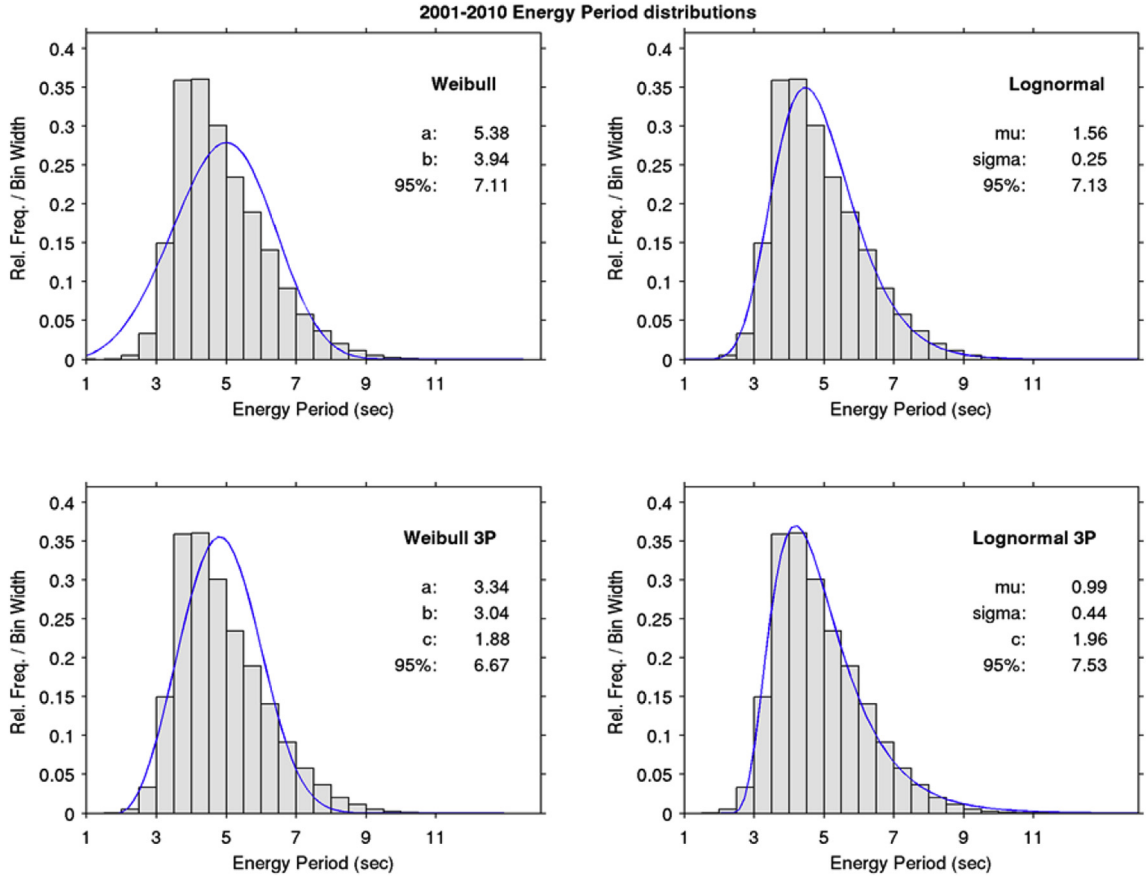

Fig. 37. Energy wave period distribution for area 2 (West of Crete).

Table 7
H_s/T_e frequency distribution (model) for the area west of Crete.

10 years: [lat:35.1 lon:23.2] 2001-2010

Te (s) \ Hs (m)	1	2	3	4	5	6	7	8	9	10	11	12
1	0	0	0	0	0	0	0	0	0	0	0	0
2	15	0	0	0	0	0	0	0	0	0	0	0
3	1701	0	0	0	0	0	0	0	0	0	0	0
4	20969	711	0	0	0	0	0	0	0	0	0	0
5	16355	12624	30	0	0	0	0	0	0	0	0	0
6	3563	13178	2346	19	0	0	0	0	0	0	0	0
7	581	4489	4556	526	11	0	0	0	0	0	0	0
8	20	1063	1735	1003	192	1	0	0	0	0	0	0
9	1	148	547	584	214	31	0	0	0	0	0	0
10	3	6	70	151	91	16	5	0	0	0	0	0
11	0	0	10	7	26	18	8	0	0	0	0	0
12	0	0	0	0	2	10	9	3	0	0	0	0

- The spatial variability of kurtosis, which is an important indicator of the impact of possible extreme values, is a basic characteristic of the area revealing the importance of high resolution studies for site selection.

Acknowledgments

The present work was supported by the MOSEP Project (Grant number 11843, 11/9/2012), which is implemented within the framework of the Action «Supporting Postdoctoral Researchers» of the Operational Program "Education and Lifelong Learning" (Action's Beneficiary: General Secretariat for Research and Technology), and is co-financed by the European Social Fund (ESF) and the Greek State.

We also acknowledge the MARINA Platform EU FP7 Project (Grant agreement number 241402) and the Atmospheric Modeling and Weather Forecasting Group of the University of Athens, for providing us the relevant atmospheric data.

References

[1] F. Ardhuin, L. Bertotti, J. Bidlot, L. Cavaleri, V. Filipetto, J. Lefevre, P. Wittmann, Comparison of wind and wave measurements and models in the Western Mediterranean Sea, Ocean. Eng. 34 (3–4) (2007) 526–541.
[2] A. Akpınar, M. Kömürcü, Assessment of wave energy resource of the Black Sea based on 15-year numerical hindcast data, Appl. Energy 101 (2013) 502–512.
[3] R. Arinaga, K.F. Cheung, Atlas of global wave energy from 10 years of reanalysis and hindcast data, Renew. Energy 39 (2012) 49–64.
[5] B. Ayat, Wave power atlas of eastern Mediterranean and Aegean seas, Energy 54 (2013), 251e262, http://dx.doi.org/10.1016/j.energy.2013.02.060.
[6] J.-R. Bidlot, Peter Janssen, Unresolved Bathymetry, Neutral Winds, and New Stress Tables in WAM, 2003. Memorandum of the Research Department R60.9/JB/0400.
[7] J. Bidlot, P. Janssen, S. Abdalla, H. Hersbach, A Revised Formulation of Ocean Wave Dissipation and its Model Impact, ECMWF Tech. Memo. 509, ECMWF, Reading, United Kingdom, 2007, p. 27. available online at, http://www.ecmwf.int/publications/.
[8] J.-R. Bidlot, Present status of wave forecasting at ECMWF, in: Proceedings from the ECMWF Workshop on Ocean Waves, 25–27 June 2012, ECMWF, Reading, United Kingdom, 2012.
[9] R. Bolaños-Sanchez, A. Sanchez-Arcilla, J. Cateura, Evaluation of two atmospheric models for wind–wave modelling in the NW Mediterranean, J. Mar. Syst. 65 (1–4) (2007) 336–353.
[10] A. Burak, A. Berna, Y. Yalçın, Black Sea wave energy atlas from 13 years hindcasted wave data, Renew. Energy 57 (2013) 436–447.
[11] F. Chiu, W. Huang, W. Tiao, The spatial and temporal characteristics of the wave energy resources around Taiwan, Renew. Energy 52 (2013) 218–221.
[12] P.C. Chu, Y. Qi, Y.C. Chen, P. Shi, Q.W. Mao, South China Sea wave characteristics. Part-1: validation of wavewatch-III using TOPEX/Poseidon data, J. Atmos. Ocean. Technol. 21 (11) (2004) 1718–1733.
[13] Z. Defne, K. Haas, H. Fritz, Wave energy potential along the Atlantic coast of the southeastern USA, Renew. Energy 34 (2009) 2197–2205.
[14] G. Emmanouil, G. Galanis, G. Kallos, L.A. Breivik, H. Heilberg, M. Reistad, Assimilation of radar altimeter data in numerical wave models: an impact study in two different wave climate regions, Ann. Geophys. 25 (3) (2007) 581–595.
[15] G. Emmanouil, G. Galanis, G. Kallos, Combination of statistical Kalman filters and data assimilation for improving ocean waves analysis and forecasting, Ocean. Model. 59–60 (2012) 11–23.
[16] G. Galanis, G. Emmanouil, G. Kallos, P.C. Chu, A new methodology for the extension of the impact in sea wave assimilation systems, Ocean. Dyn. 59 (3) (2009) 523–535.
[17] G. Galanis, P.C. Chu, G. Kallos, Statistical post processes for the improvement of the results of numerical wave prediction models. A combination of Kolmogorov-Zurbenko and Kalman filters, J. Operat. Oceanogr. 4 (1) (2011) 23–31.
[18] G. Galanis, D. Hayes, G. Zodiatis, P.C. Chu, Y.H. Kuo, G. Kallos, Wave height characteristics in the Mediterranean Sea by means of numerical modeling, satellite data, statistical and geometrical techniques, Mar. Geophys. Res. 33 (2012) 1–15.
[19] M. Gonçalves, P. Martinho, C.G. Soares, Wave energy conditions in the western French coast, Renew. Energy 62 (2014) 155–163.
[20] M. Hughes, A. Heap, National-scale wave energy resource assessment for Australia, Renew. Energy 35 (8) (2010) 1783–1791.
[21] G. Iglesias, R. Carballo, Wave energy resource along the Death Coat (Spain), Renew. Energy 34 (2009) 1963–1975.
[22] G. Iglesias, M. Lopez, R. Carballo, A. Castro, J.A. Fraguela, P. Frigaard, Wave energy potential in Galicia (NW Spain), Renew. Energy 34 (2009) 2323–2333.
[23] G. Iglesias, R. Carballo, Wave energy resource in the Estaca de Bares area (Spain), Renew. Energy 35 (2010) 1574–1584.
[24] N. Jadidoleslam, M. Ozger, N. Agıralioglu, Wave power potential assessment of Aegean Sea with an integrated 15-year data, Renew. Energy 86 (2016) (2016) 1045–1059.
[25] J. Janeiro, F. Martins, P. Relvas, Towards the development of an operational tool for oil spills management in the algarve coast, J. Coast. Conserv. 16 (4) (2012) 449–460.
[26] Z.I. Janjic, Nonlinear advection schemes and energy cascade on semi-

staggered grids, Mon. Weather Rev. 112 (1984) 1234–1245.
[27] P. Janssen, P. Lionello, M. Reistad, A. Hollingsworth, A Study of the Feasibility of Using Sea and Wind Information from the ERS-1 Satellite, Part 2: Use of Scatterometer and Altimeter Data in Wave Modelling and Assimilation, 1987 (ECMWF report to ESA, Reading).
[28] P. Janssen, ECMWF wave modeling and satellite altimeter wave data, in: D. Halpern (Ed.), Satellites, Oceanography and Society, Elsevier, 2000, pp. 35–36.
[29] P.A.E.M. Janssen, M. Onorato, The intermediate water depth limit of the Zakharov equation and consequences for wave prediction, J. Phys. Oceanogr. 37 (2007) 2389–2400.
[30] Joana C.C. van Nieuwkoop, Helen C.M. Smith, George H. Smith, Lars Johanning, Wave resource assessment along the Cornish coast (UK) from a 23-year hindcast dataset validated against buoy measurements, Renew. Energy 58 (2013) 1–14.
[31] G. Kallos, The Regional weather forecasting system SKIRON, in: Proceedings, Symposium on Regional Weather Prediction on Parallel Computer Environments, 15–17 October 1997, Athens, Greece, 1997, p. 9.
[32] G. Kallos, P.J. Athanasiadis, G. Galanis, C. Mitsakou, S. Sofianos, G.A. Athanassoulis, C. Spyrou, C. Kalogeri, Energy Resource Mapping in the Framework of the MARINA PLATFORM Project, European Geosciences Union, 2011.
[33] E. Kalnay, Atmospheric Modeling, Data Assimilation and Predictability, Cambridge University Press, 2002, p. 341.
[34] G. Komen, L. Cavaleri, M. Donelan, K. Hasselmann, S. Hasselmann, P. Janssen, Dynamics and Modelling of Ocean Waves, Cambridge University Press, 1994.
[35] J.M. Leishman, G. Scobie, The Development of Wave Power – A Techno Economical Study, Dept. of the industry, 1976. NEL Report, EAU M25.
[36] P. Lionello, H. Günther, P. Janssen, Assimilation of altimeter data in a global third generation wave model, J. Geophys. Res. 97 (C9) (1992) 14453–14474.
[37] A.C. Lorenc, A global Three-dimensional Multivariate Statistical interpolation scheme, MonthlyWeatherReview 109 (1981) 701–721.
[38] L. Magnusson, A. Thorpe, M. Bonavita, S. Lang, T. McNally, N. Wedi, Evaluation of Forecasts for Hurricane Sandy, Technical Memorandum, No. 699, ECMWF, 2013.
[39] N. Mazarakis, V. Kotroni, K. Lagouvardos, L. Bertotti, High-resolution wave model validation over the greek maritime areas, Nat. Hazards Earth Syst. Sci. 12 (11) (2012). http://dx.doi.org/10.5194/nhess-12-3433-2012.
[40] F. Mesinger, A blocking technique for representation of mountains in atmospheric models, Riv. Meteorol. Aeronaut. 44 (1984) 195–202.
[41] N. Mori, P.A.E.M. Janssen, On kurtosis and occurrence probability of freak waves, J. Phys. Oceanogr. 36 (2006) 1471–1483.
[42] S. Musič, S. Nickovič, 44-year wave hindcast for the Eastern Mediterranean, Coast. Eng. 55 (2008) 872–880.
[43] A. Papadopoulos, P. Katsafados, G. Kallos, Regional weather forecasting for marine application, Glob. Atmos. Ocean. Syst. 8 (2–3) (2001) 219–237.
[44] A. Papadopoulos, P. Katsafados, Verification of operational weather forecasts from the POSEIDON system across the Eastern Mediterranean, Nat. Hazards Earth Syst. Sci. 9 (2009) 1299–1306.
[45] M.T. Pontes, Assessing the European wave energy resource, Trans. Am. Meteorol. Soc. 120 (1998) 226–231.
[47] S.T. Rao, I.G. Zurbenko, R. Neagu, P.S. Porter, J.Y. Ku, R.F. Henry, Space and time scales in ambient ozone data, Bull. Amer. Meteor. Soc. 78 (10) (1997) 2153–2166.
[48] A.W. Ratsimandresey, M.G. Sotillo, J.C. Carretero, E. Alvarez, H. Hajji, A 44-year high-resolution ocean and atmospheric hindcast for the Mediterranean basin developed within the HIPOCAS project, Coast. Eng. 55 (2008) 827–842.
[49] G. Reikard, P. Pinson, J.R. Bidlot, Ocean. Eng. 38 (10) (2011) 1089–1099.
[50] L. Rusu, Guedes Soares, Wave energy assessments in the Azores islands, Renew. Energy 45 (2012) 183–196.
[51] J. Stopa, K. Cheung, Y.L. Chen, Assessment of wave energy resources in Hawaii, Renew. Energy 36 (2) (2011) 554–567.
[52] J. Stopa, K. Cheung, H. Tolman, Patterns and cycles in the climate forecast system reanalysis wind and wave data, Ocean. Model. 70 (2013).
[53] WAMDIG, The WAM-Development and Implementation Group, S. Hasselmann, K. Hasselmann, E. Bauer, L. Bertotti, C.V. Cardone, J.A. Ewing, J.A. Greenwood, A. Guillaume, P. Janssen, G. Komen, P. Lionello, M. Reistad, L. Zambresky, The WAM Model – A third generation ocean wave prediction model, J. Phys. Oceanogr. 18 (12) (1988) 1775–1810.
[54] D. Vicinanza, P. Contestabile, V. Ferrante, Wave energy potential in the north-west of Sardinia (Italy), Renew. Energy 50 (2013) 506–521.
[55] T. Soomere, M. Eelsalu, On the wave energy potential along the eastern Baltic Sea coast, Renew. Energy 71 (2014) 221–233.